High-Temperature Nano-Derived Micro-H_2 and -H_2S Sensors

Christina Wildfire, Engin Ciftyurek, Edward M. Sabolsky

Energy Materials Program
Department of Mechanical and Aerospace Engineering
West Virginia University

Annual DOE-NETL University Coal Research Project Review
May 30-31, 2012

Outline

- Objectives
- Background and proposed work plan
- Synthesis of nanomaterials
- Evaluation of H_2 nanomaterials
- Micro-patterning techniques
- Stable micro-interdigitized electrodes (µIDEs)
- Conclusions
- Future Work

Objectives

- Develop micro-scale, chemical sensors composed of nano-derived, metal-oxide materials which display stable performance within high-temperature environments (>500°C).
- Short term– Develop high-temperature H_2 and H_2S sensor using low cost, easily reproducible methods with 3D porous nanomaterials.
- Long term – Develop high-temperature micro-sensor arrays to detect gases such as NO_x, SO_x, H_2S, H_2, HCs.
- Collaboration with NexTech Materials, Ltd. (Lewis Center, OH).

Proposed Work Plan

Task 2.0 Synthesis and Characterization of Nano-Composite Electrodes. Doped-tin oxide, ceria and zirconate (perovskite and pyrochlore) nanomaterials will be synthesized using hydrothermal and/or glycine-nitrate processes and characterized.

Task 3.0 Lost-Mold Microcasting of the Selective Electrode Structure. Develop microcasting methods for patterning microscale, chemically selective pads on alumina wafers.

Task 4.0 Fabrication of Micro-Sensors and Arrays. Fabricate functional hydrogen micro-sensors and micro-sensor arrays. In addition, stable IDEs for high-temperature applications must be developed.

Task 5.0 Micro-Sensor and Sensor Array Testing.

Micro-sensors will be first characterized for baseline resistance using external furnace heat at temperatures ranging from 500°C to at least 1100°C. Key tests include:

- *Hydrogen sensitivity and selectivity*
- *Humidity sensitivity (0-10% H_2O)*
- *O_2 requirements (0.1-20%)*
- *CO cross-sensitivity (ppm-% CO)*
- *Temperature sensitivity (500-1200°C)*
- *Poison effects (<200 ppm PH_3, H_2S, HCl)*

Proposed Work Schedule

Schedule of tasks and milestones												
Task/*Milestone*	**Quarter after Project Initiation**											
	1	**2**	**3**	**4**	**5**	**6**	**7**	**8**	**9**	**10**	**11**	**12**
Task 1. Project Management and Planning (Q1-Q12)												
Subtask 1.1: Kick-Off Meeting and Sensor Design at WVU.												
→ *MS: Sensor and Array Established*		▲										
Subtask 1.2: Project Meetings and Reporting												
→ *DL: Quarterly Reports*	●	●	●	●	●	●	●	●	●	●	●	●
→ *DL: Annual Progress Reports*				●				●				
→ *DL: Final Technical Report*												●
Task 2. Synthesis and Characterization of Nano-Composite Electrodes. (Q1-Q7)												
Subtask 2.1: Synthesis of Zirconate Electrode Compositions												
→ *MS: Process for synthesizing ABO_3 and $A_2B_2O_7$ nano-powder established*				▲								
Subtask 2.2: Composite Selective Electrodes												
→ *DL: NexTech nano-catalyst delivered to WVU for stability testing*			●									
Subtask 2.3: Electrode Characterization												
→ *MS: Stability of H_2 and H_2S nano-composites electrodes defined to 1200℃*						▲						
Task 3. Lost-Mold Microcasting of the Selective Electrode Structure. (Q5-Q11)												

Task/*Milestone*	Quarter after Project Initiation											
	1	2	3	4	5	6	7	8	9	10	11	12
Task 3. Lost-Mold Microcasting of the Selective Electrode Structure. (Q5-Q11)												
Subtask 3.1: Micro-Mold Fabrication												
→ *MS: Microcasting process defined*						▲						
→ *DL: Micro-molds delivered to NexTech for commercial microcasting demonstration*					●	●	●	●				
Subtask 3.2: Lost-Mold Microcasting and Sintering of Micro-Selective Electrode												
Subtask 3.3: Selective Electrode (SE) Characterization.												
Task 4. Fabrication of Micro-Sensors and Arrays (Q6-Q12)												
Subtask 4.1: Pt Interconnect and Counter-Electrode (CE) Deposition												
Subtask 4.2: Selective Electrode (SE) Deposition/Sintering												
→ *MS: Micro-sensor fabricated*								▲				
Subtask 4.3: H_2-H_2S Micro-Sensor Array Fabrication												
→ *MS: Micro-sensor array fabricated*									▲			
Task 5. Micro-Sensor and Sensor Array Testing (Q8-Q12)												
Subtask 5.1: Testing of H_2 micro-sensors												
→ *MS: Micro-sensor specification targets achieved*											▲	
→ *DL: Delivery of sensors to NexTech for testing*							●	●	●	●	●	
Subtask 5.2: Testing of H_2S micro-sensors and H_2-H_2S array												
→ *MS: Micro-sensor array specification targets achieved*												▲

Proposed Milestones

- Sensor and Sensor Array design established – **Q2**
- Process for synthesizing nanomaterials established – **Q4**
- Stability of H_2 and H_2S nano-composites electrodes defined to 1200°C – **Q6**
- Micro-casting process defined – **Q6**
- Micro-sensors fabricated – **Q8**
- Micro-sensor array fabricated – **Q9**
- Micro-sensor specification targets achieved – **Q11**
- Micro-sensor array specification targets achieved – **Q12**

Proposed Deliverables

1) Quarterly and annual progress reports to DOE

2) Subtask 2.2- industrial partner delivers nanomaterials to WVU for stability testing (Q3)

3) Subtask 3.1- Micro-molds delivered to industrial partner for commercial microcasting demonstration ***(Q5-8)***

4) Subtask 5.1- Delivery of micro-sensors to industrial partner for testing ***(delivery start of each quarter Q7-Q11)***

5) Subtask 5.2- Delivery of arrays to industrial partner for testing ***(delivery start of each quarter Q7-Q12)***

Presentations of this Work

1. "High temperature nano-derived hydrogen sensors," Christina Wildfire, Engin Ciftyurek, Katarzyna Sabolsky, Edward M. Sabolsky, European Ceramics Society (ECerS) XII conference in Stockholm, Sweden, June 19-23 2011, Nanomaterials Symposium; **INVITED PRESENTATION**
2. "Performance and Stability of High-Temperature Nano-Derived Hydrogen Sensors," Edward M. Sabolsky, Christina Wildfire, Engin Ciftyurek, Katarzyna Sabolsky, 220th Electrochemical Society Meeting, Boston, MA, Oct. 9-14, 2012; **PRESENTATION**
3. "High-Temperature Nanomaterials for Electrochemical Micro-Sensors," Edward M. Sabolsky, Christina Wildfire, Engin Ciftyurek, Energy Materials and Applications (EMA) 2012 Conference in Orlando, FL, January 18-20, 2012, S1: New Frontiers in Electronic Ceramic Structures, Advanced Electronic Material Devices and Circuit Integration; **PRESENTATION**
4. "Nano-Derived, Micro-Chemical Sensors for High-Temperature Applications," Edward M. Sabolsky, Christina Wildfire, Engin Ciftyurek, Katarzyna Sabolsky, 221st Electrochemical Society Meeting in Seattle, WA, May 6-10, 2012; **INVITED PRESENTATION**
5. "High-Temperature Nano-Derived Chemical Micro-Sensors," Edward M. Sabolsky, Christina Wildfire, Engin Ciftyurek, Katarzyna Sabolsky, 10th International Symposium on Ceramic Materials and Components for Energy and Environmental Applications (CMCEE) 2012 in Dresden, Germany, May 20-23, 2012; **PRESENTATION**

Publications of this Work

1. "Nano-Derived, Micro-Chemical Sensors for High-Temperature Applications," E.M. Sabolsky, C. Wildfire, E. Ciftyurek, K. Sabolsky, ECS Transactions, 45 (3) 495-506 (2012).
2. "Platinum Thin Film Electrodes for High Temperature MEMs Applications," E. Ciftyurek, K. Sabolsky, E. M. Sabolsky, *Journal of Microelectromechanical Systems*, Submitted in April 2012
3. "Functionally Gradient Zr-Pt Composite Thin Films for Stable High-Temperature Electrodes," E. Ciftyurek, K. Sabolsky, E. M. Sabolsky, *Thin Solid Films*, to be submitted in June 2012
4. "Investigatoin of Lanthanum Zirconate Pyrochlores for High Temperature Hydrogen Sensing," Christina Wildfire, Edward M. Sabolsky, Engin Ciftyurek, Katarzyna Sabolsky, Sensors and Actuators B, To be submitted in June

5. "High Temperature Semiconducting Hydrogen Sensors Based on Lanthanum Tinanate Materials," Christina Wildfire, Edward M. Sabolsky, Engin Ciftyurek, Katarzyna Sabolsky, Sensors and Actuators B, To be submitted in June

6. "Development and Testing of High Temperature Hydrogen Micro-Sensors," Christina Wildfire, Edward M. Sabolsky, Engin Ciftyurek, Katarzyna Sabolsky, Sensors and Actuators B, To be submitted in June

Sensor Background

Background- Chemiresistive Sensors

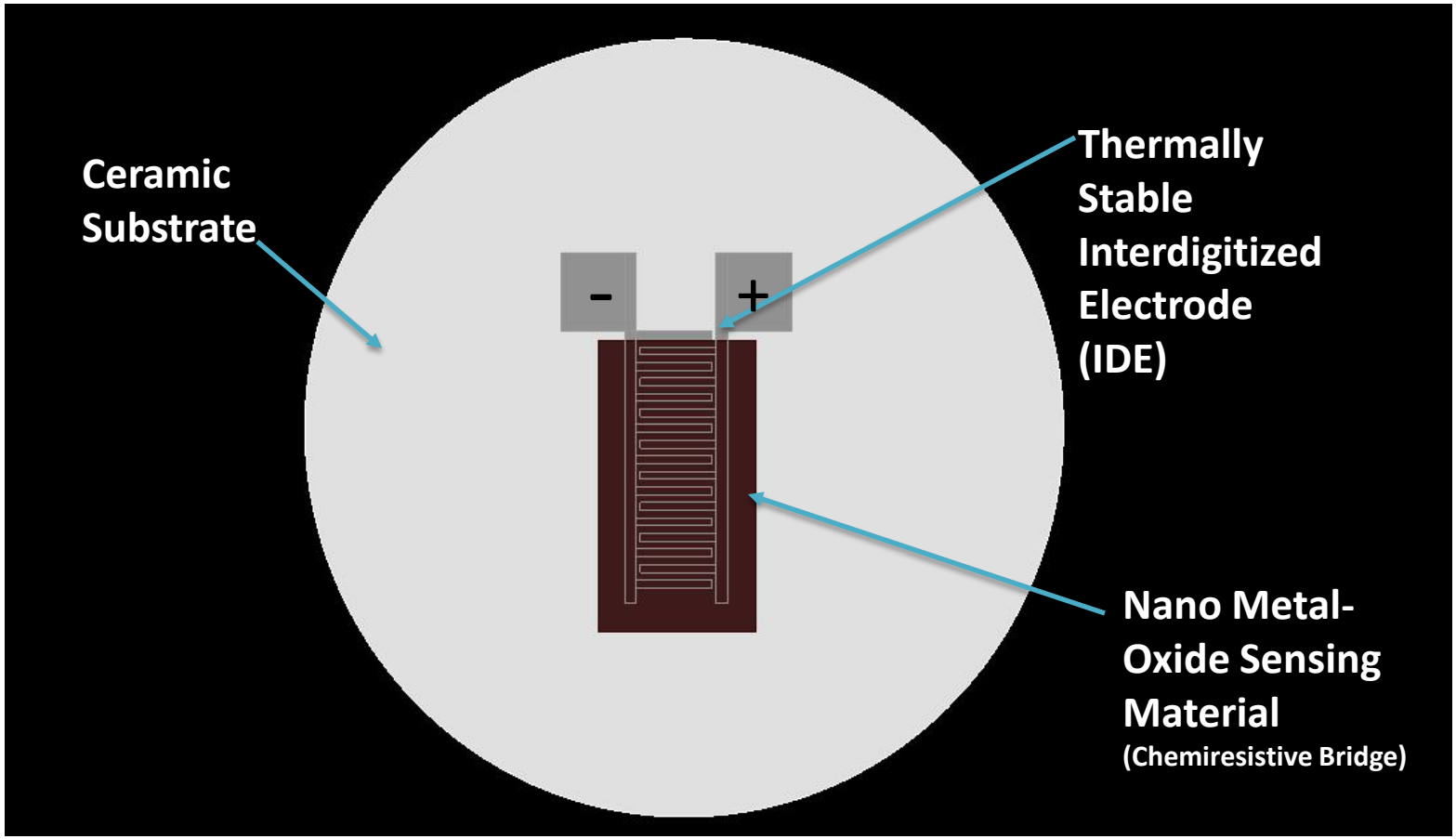

- Metal-oxide's shape, size, composition, and surface characteristics controls the selectivity and sensitivity.
- Nanomaterials provide ultra-high surface area which will enhance encounter of chemical species with sensing material.

Current High-Temp H_2 Sensors

- Industrial applications above 500˚C
- Special interest from DOE for harsh environment sensors (turbine engines, gasifiers, etc)
- Not for RT and ambient safety purposes
- Example of industrial environment

Slagging gasifier :
(at 1315°C exit)

39.2% H_2, **40.3 % CO**, 0.11% CH_4, 17.3% CO_2, 0.87% H_2S+Sulfides, 0.41% H_2O, **0.78% O_2** *

*Ind. Eng. Chem. Res. 50 [3], 1674 (2011)

Refractory Nanomaterials

Pyrochlore $A_2B_2O_7$ (focus on A= Gd and B=Zr, Sn, Ti)

- **Not prone to carbonate formation or CO adsorption (i.e. low CO interference).**
- **Dopants in A-site (Sm, Y, Yb, Ca, Sr….) increase $V_O^{\cdot\cdot}$ concentration, and thus, ionic conductivity.**
- **Mixed-ionic conductor (O^{2-} and H^+ conduction).**
- **Humidity required for proton conduction.**
- **Ionic and electronic contribution can be controlled by substitution and oxygen partial pressure.**
- ***Highly resistant to sintering and coarsening***

Sensing Mechanisms

Ionic Conductor

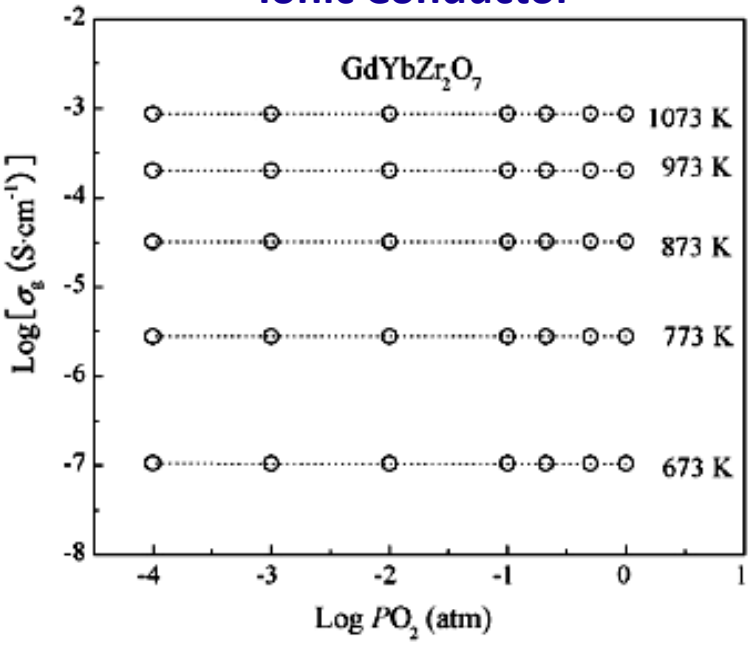

Liu et al. J. Alloys and Compounds 490, 277 (2010).

n-Type Conductor

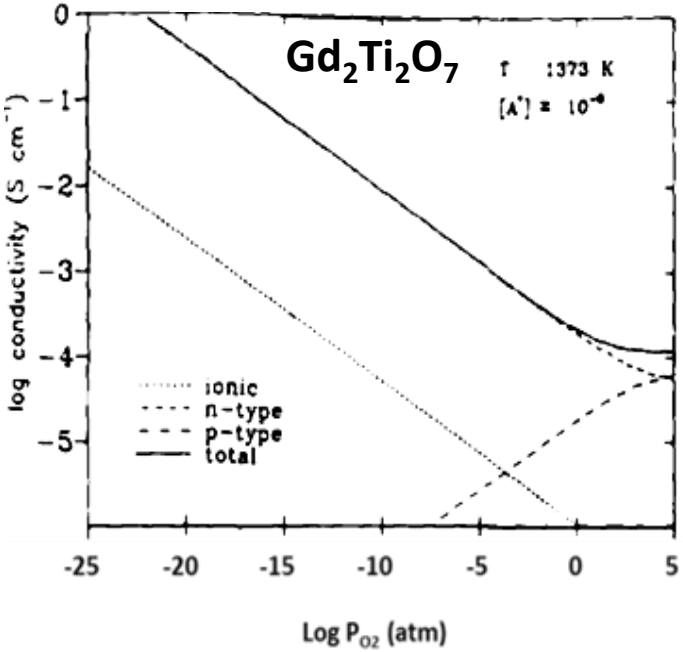

Tuller, Solid State Ionics (1992)

$Gd_2Zr_2O_7$ (Ionic) → $Gd_2Zr_2O_7 - SnO_2$ (Ionic – Semiconductor) composite → $Gd_2(Zr_xSn_{(1-x)})_2O_7$ (mixed conduction) solid solution → $Gd_2Ti_2O_7$ (Mixed Semiconductor)

Nanomaterial Synthesis and Sensor Testing

Synthesis of Nanomaterials

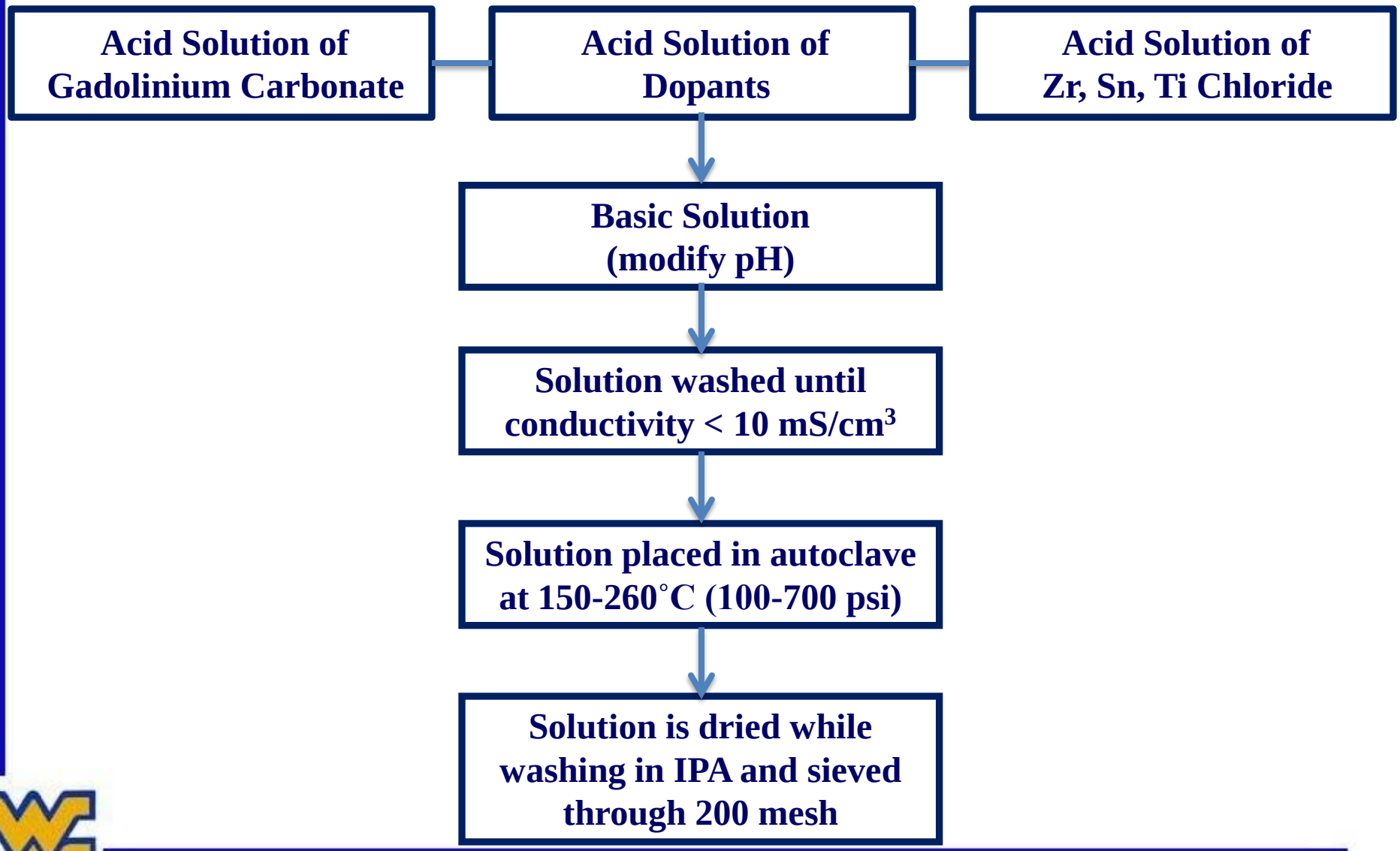

Structural Characterization (XRD)

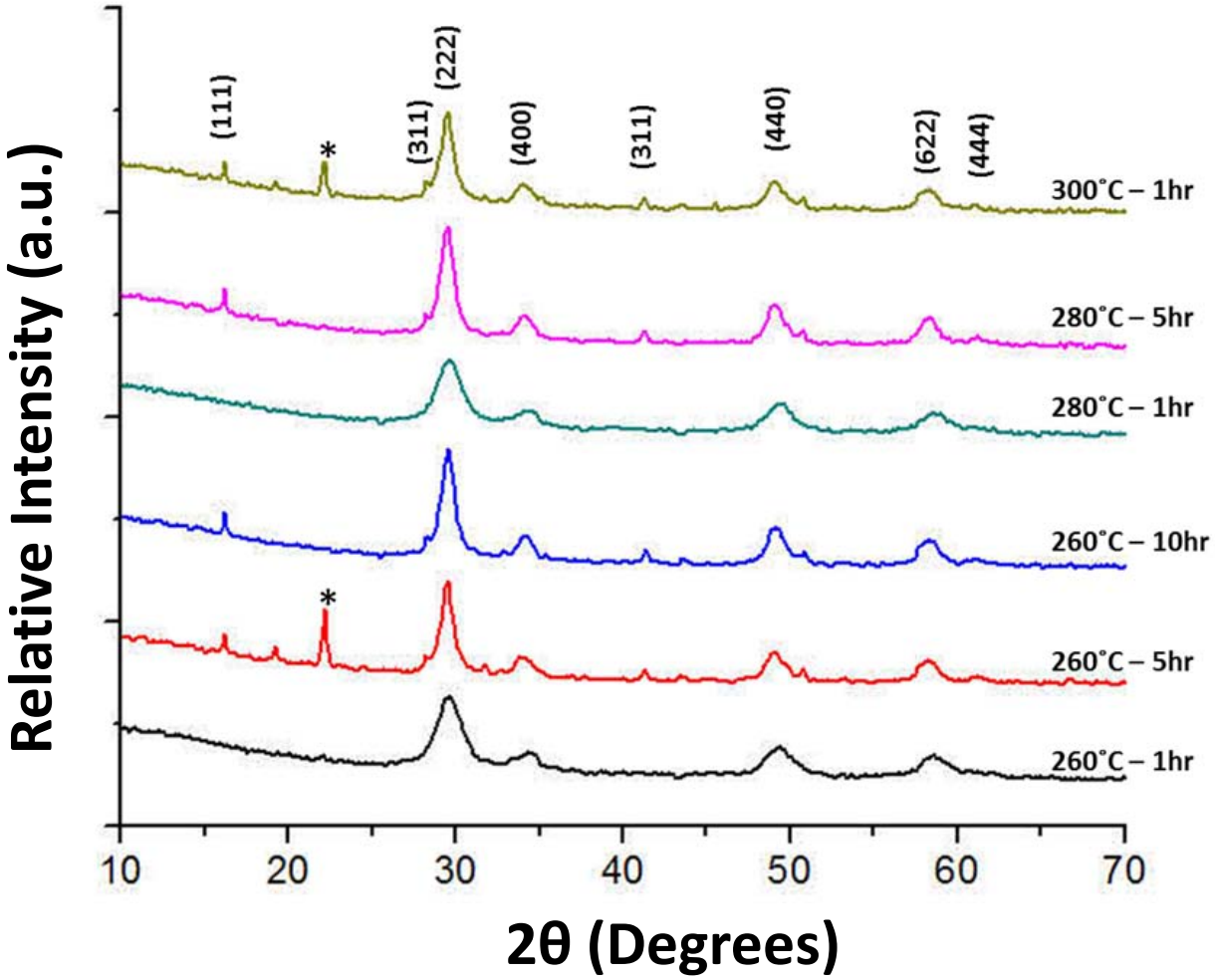

$Gd_{1.8}Y_{0.1}Zr_2O_7$

pH=11

- Higher temps or longer dwell times needed for pyrochlore phase
- Broad peaks due to particle sizes in nano range

* TMAOH

Structural Characterization (XRD)

$Gd_2Sn_2O_7$

- pH was adjusted from 6 to 11
- pH>8 creates secondary phase of $Gd(OH)_3$
- pH=6 creates single pyrochlore phase

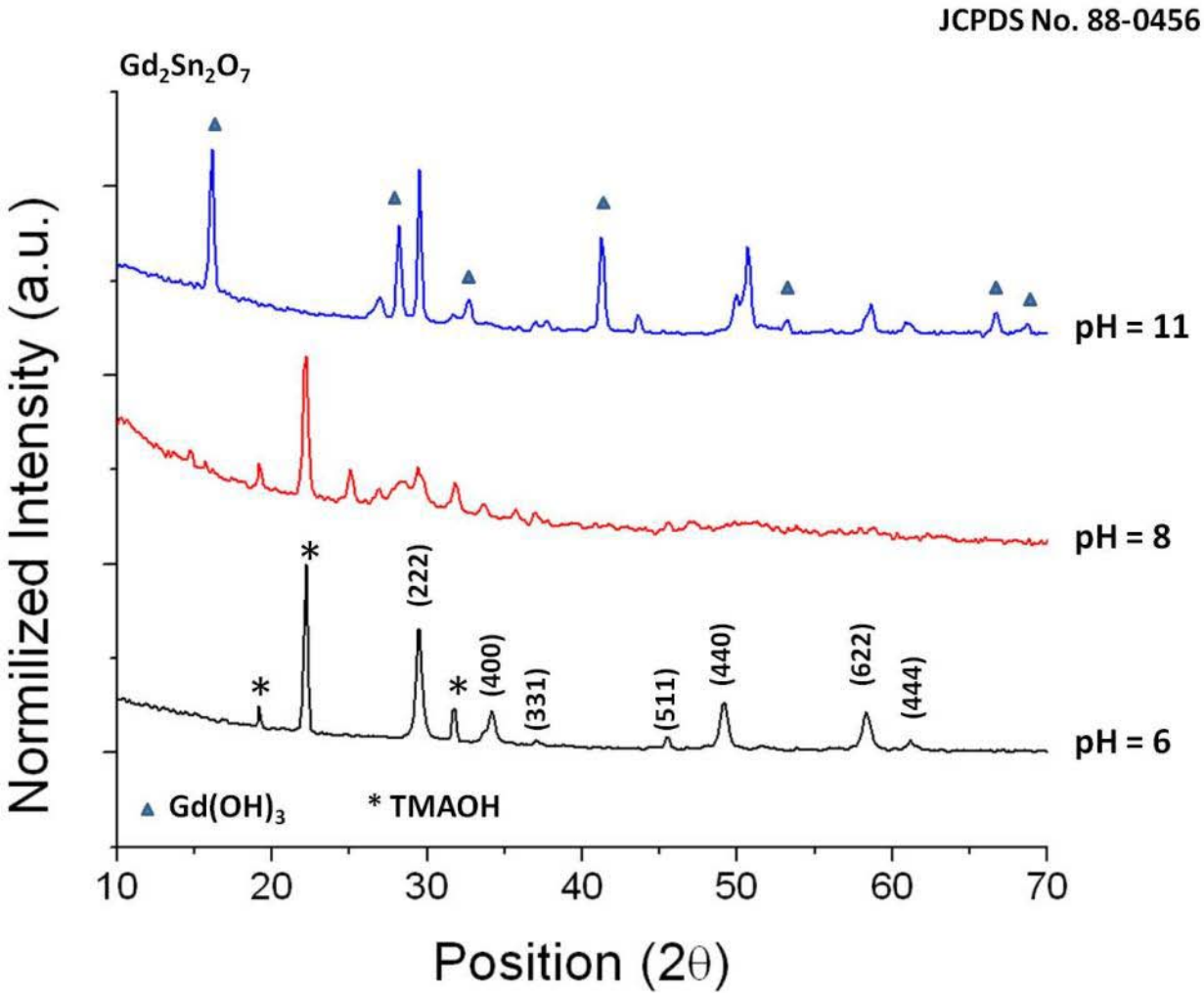

Thermal Stability of Nano-GZ

- Particle size increases from 4 nm to <70 nm.
- Structure necks at 1200˚C, but nano-network remains highly porous (nanoporous).

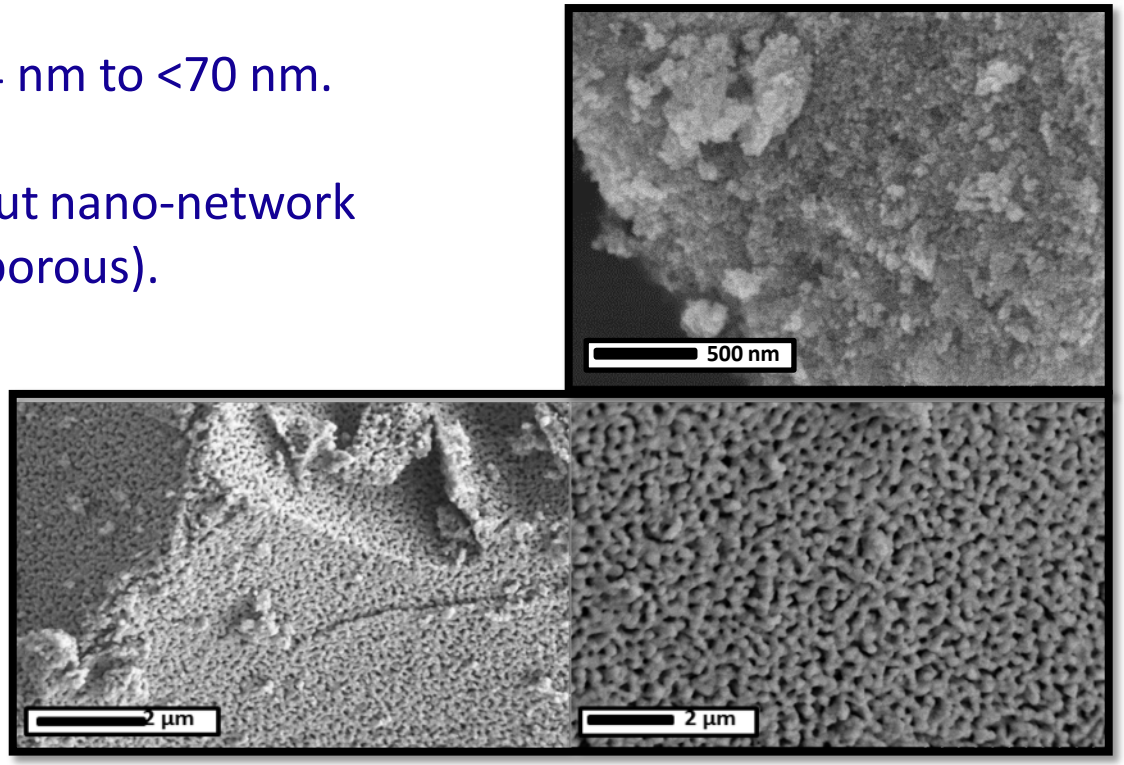

Calcined 1200˚C for 10 hours

	Sintered 1 Hour	Sintered 24 Hours
BET Surface Area	3.5 m^2/g (244nm)	3.6 m^2/g (234nm)
Adsorption SA of pores	2.639 m^2/g	2.793 m^2/g
Volume of pores (adsorption)	0.0107 cm^3/g	0.00654 cm^3/g

Compositional Testing Protocol

Macro-Sensor Fabrication:

- Alumina substrates polished
- Pt-IDEs sputtered and annealed at 1200˚C
- Sensing material printed onto electrodes and sintered at 1200˚C (~80-100 µm thick)

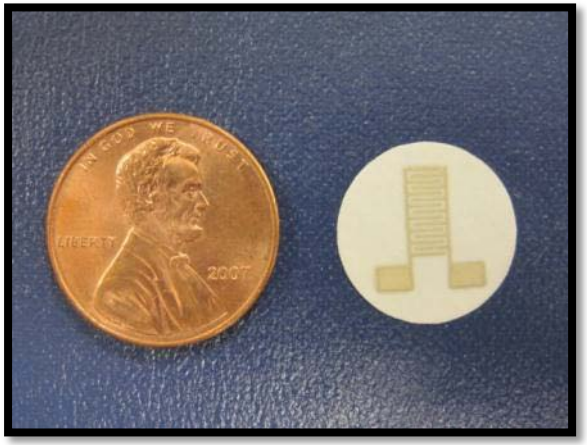

Screenprinted Electrode (250 µm finger spacing)

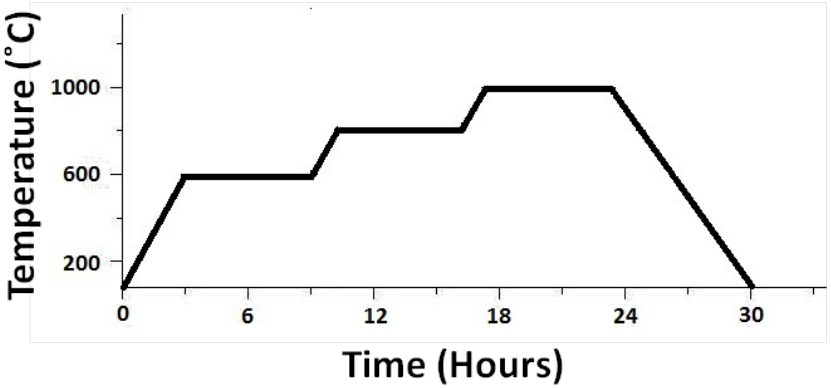

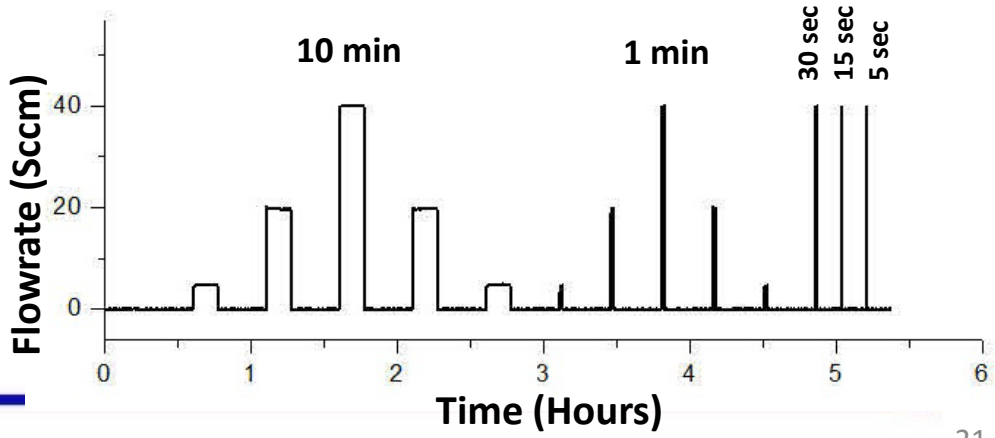

Macro-Sensor Testing (SnO_2)

WVU Nano-SnO_2 Ordered Agglomerates

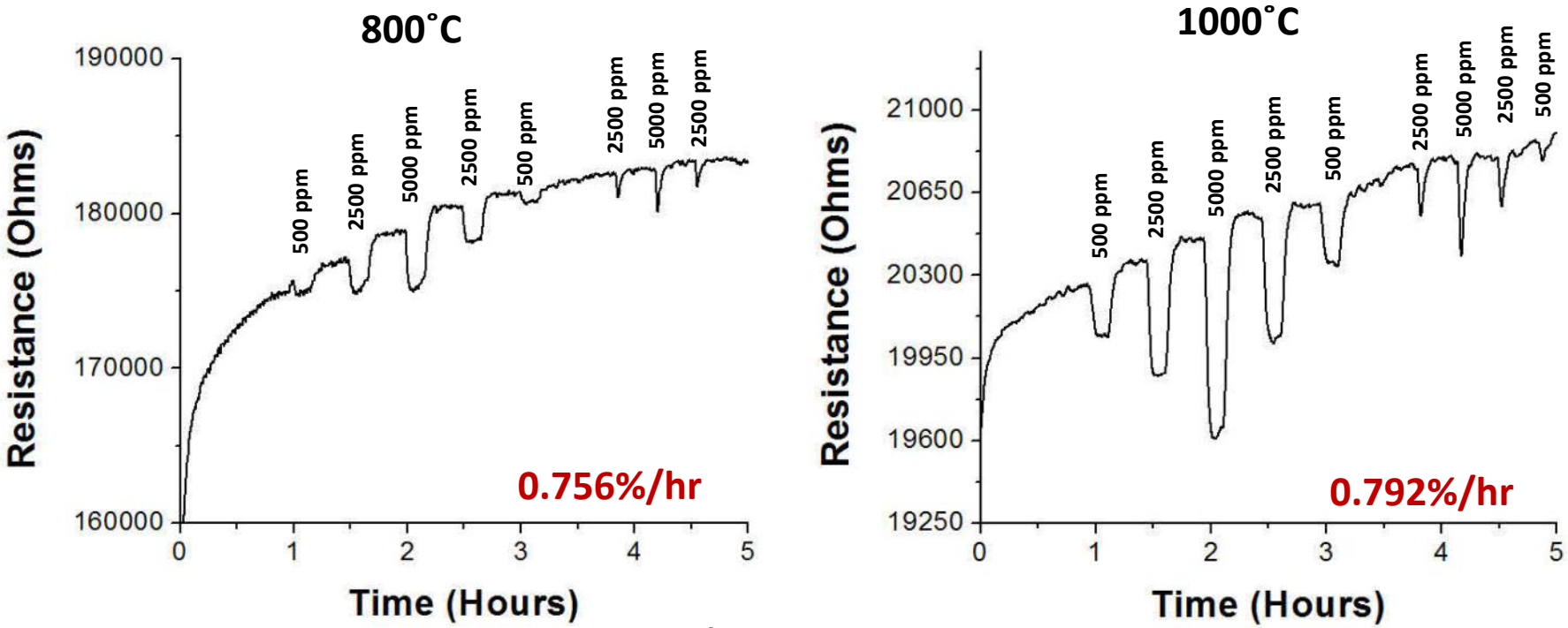

H_2/N_2, 20% Oxygen

- WVU nano-SnO_2 has high level of sensitivity to ppm levels of H_2 at higher temperatures.
- Degradation or "drift" in sensor due to sintering/coarsening (3 nm to ~0.5 μm).

Macro-Sensor Testing ($Gd_{2-x}A_xZr_2O_7$)

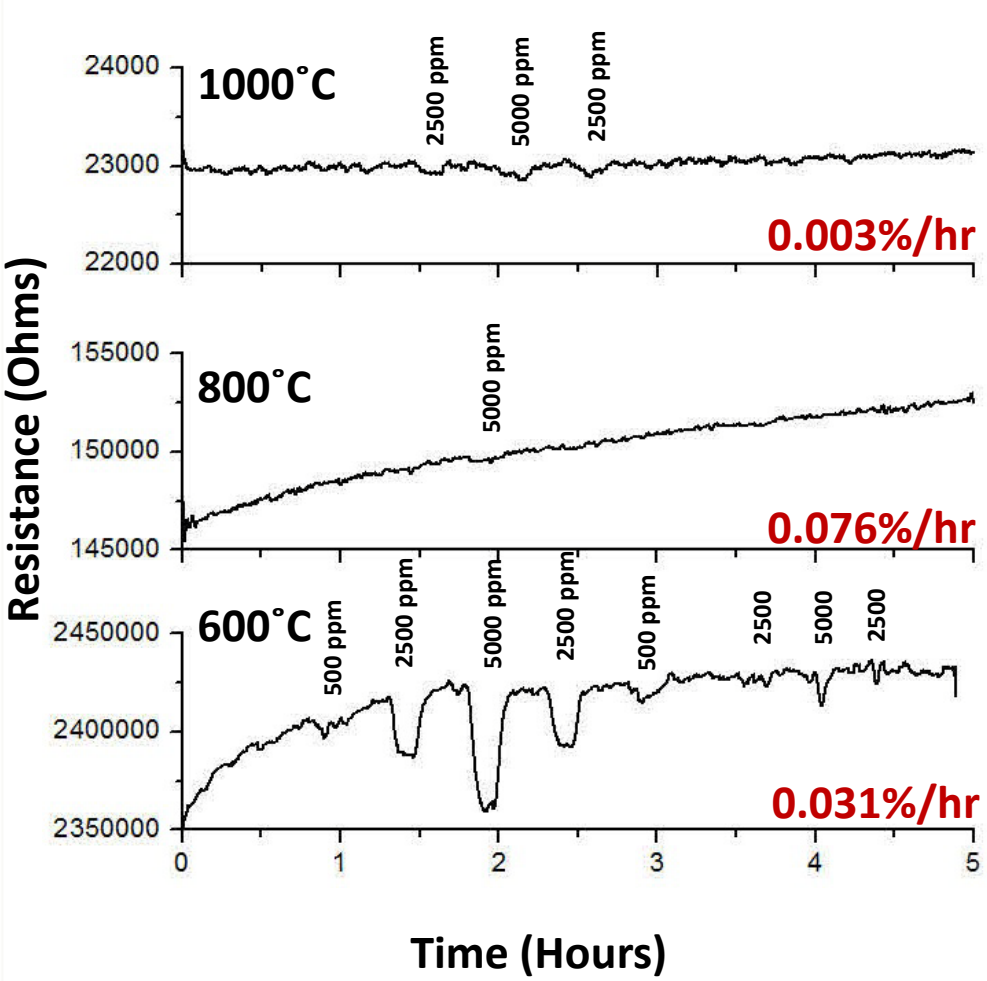

- Doped zirconate sensor shows sensitivity to H_2 in air at 600°C (no humidity).
- Surface reduction at lower temperature results in n-type dominated response.
- Steam formation dominates at higher temperature (low H_2 adsorption and reaction with zirconate surface).

H_2/N_2, ***20% Oxygen***

Compositional Testing ($50\%\ SnO_2$-$50\%Gd_{1.8}Y_{0.1}Zr_2O_7$)

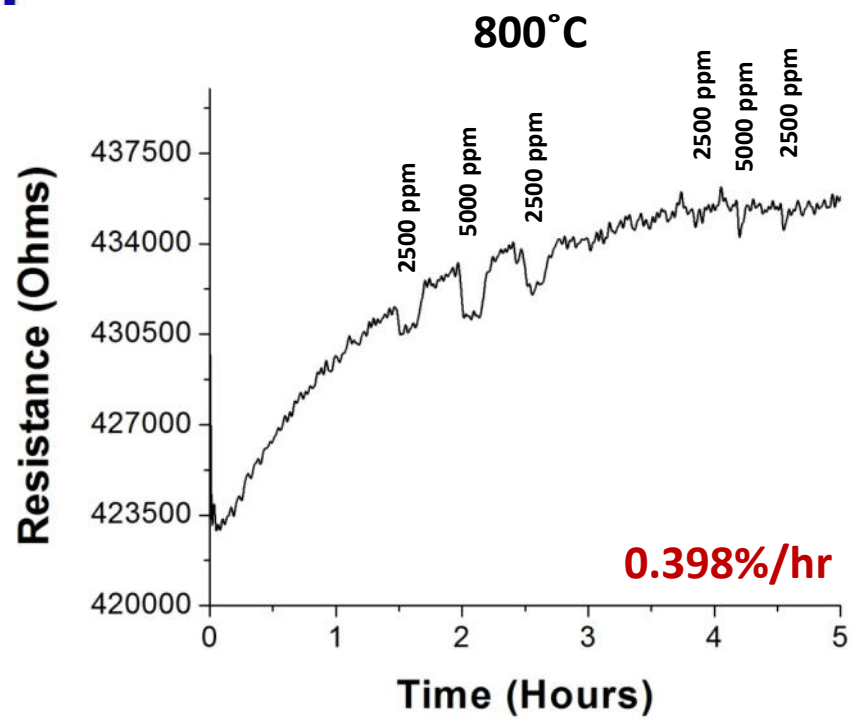

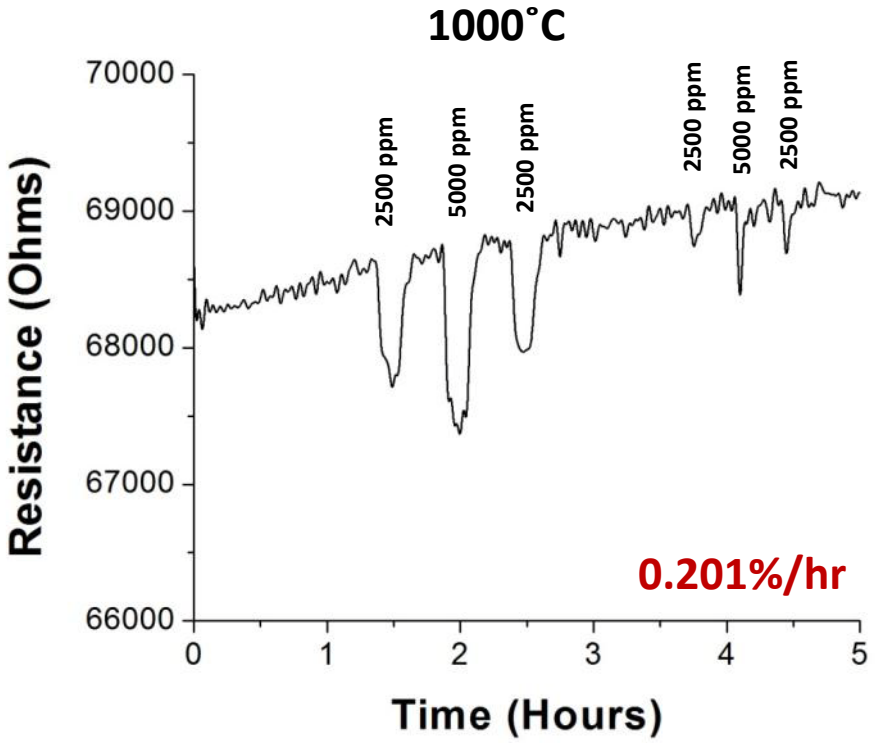

H_2/N_2, *20% Oxygen*

- Dispersed nano-suspensions combined to make composite.
- Addition of SnO_2 allows for H_2 adsorption at higher temperatures.
- Zirconate limits amount of "drift" seen throughout testing.

Compositional Testing

(10%-SnO_2-90%-$Gd_{1.8}Y_{0.1}Zr_2O_7$)

1000°C

- SnO_2 increases H_2 adsorption.
- Surface O^- reaction or O_o^x junction reduction leads to n-type like response.

- Decreased ionic conduction across contact junctions.
- Enough oxygen in atmosphere for reaction without assistance from bulk

- Vacancy conc. change at contacts.
- Oxygen/vacancy diffusion into bulk increases conductivity to cause Ω relaxation.

- Stabilization change is limited due to available oxygen.

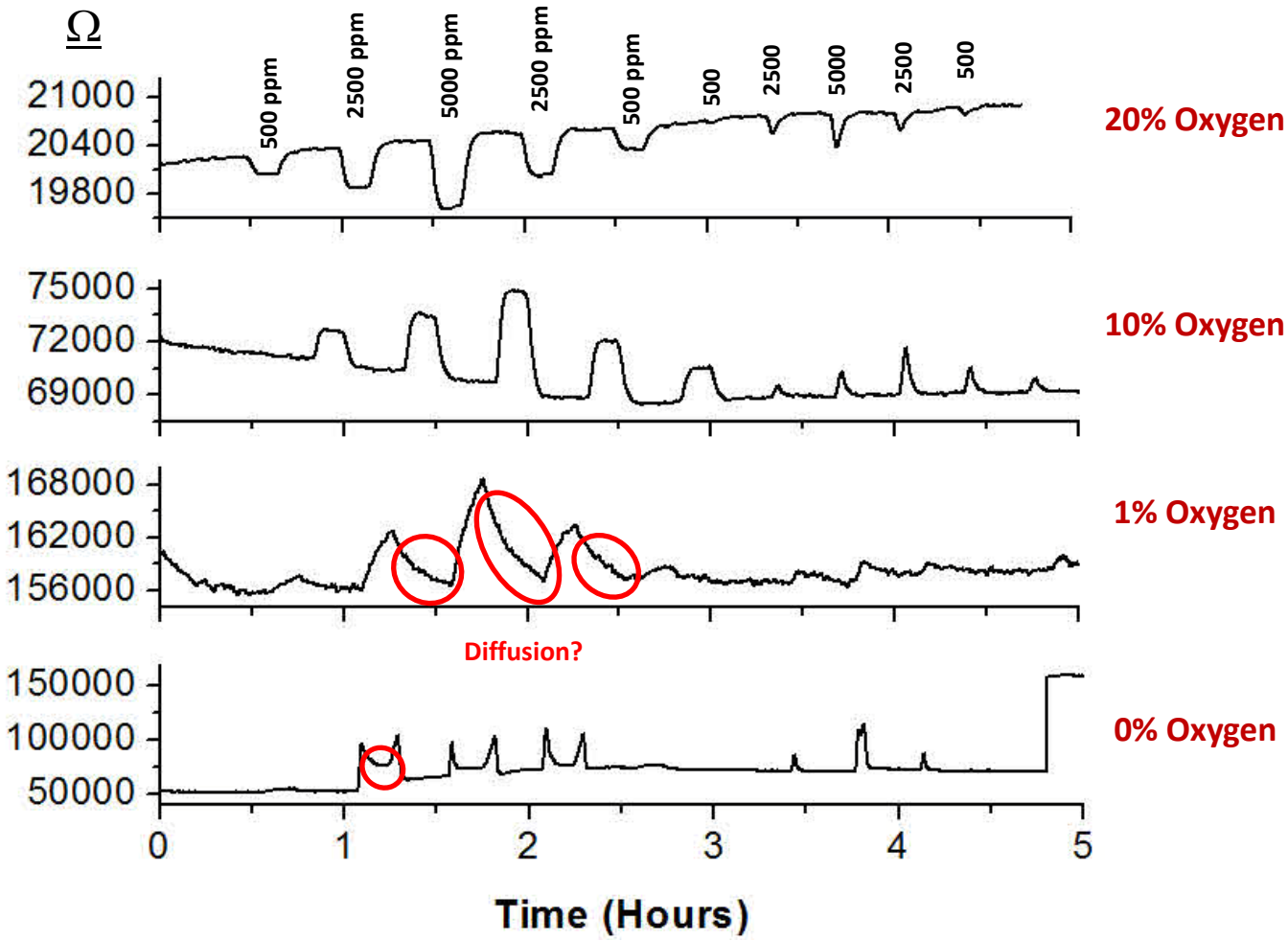

No Humidity

Comparison of Composite Sensors

20% Oxygen Atmosphere

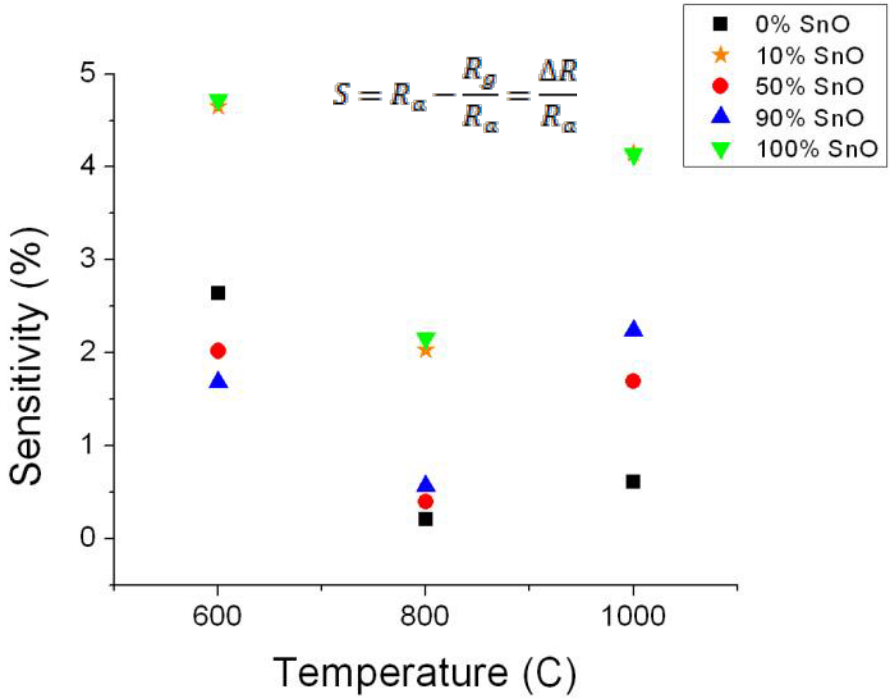

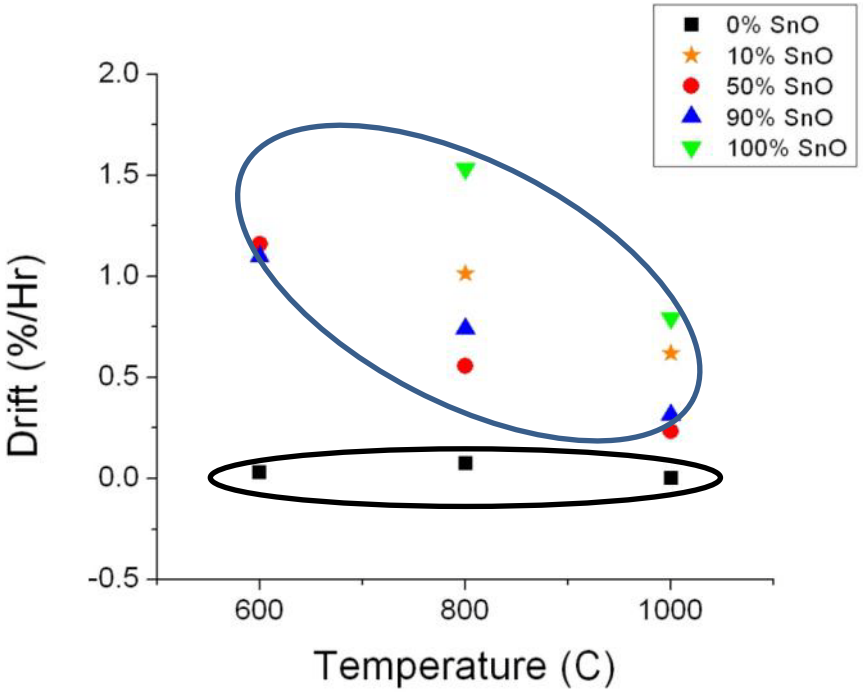

- Addition of SnO_2 increases sensitivity at elevated temperatures but decreases stability as temperature increases
- 10% SnO_2 composite shows more sensitivity than composites with higher % of SnO_2

Comparison of Sensing Materials

20% Oxygen Atmosphere

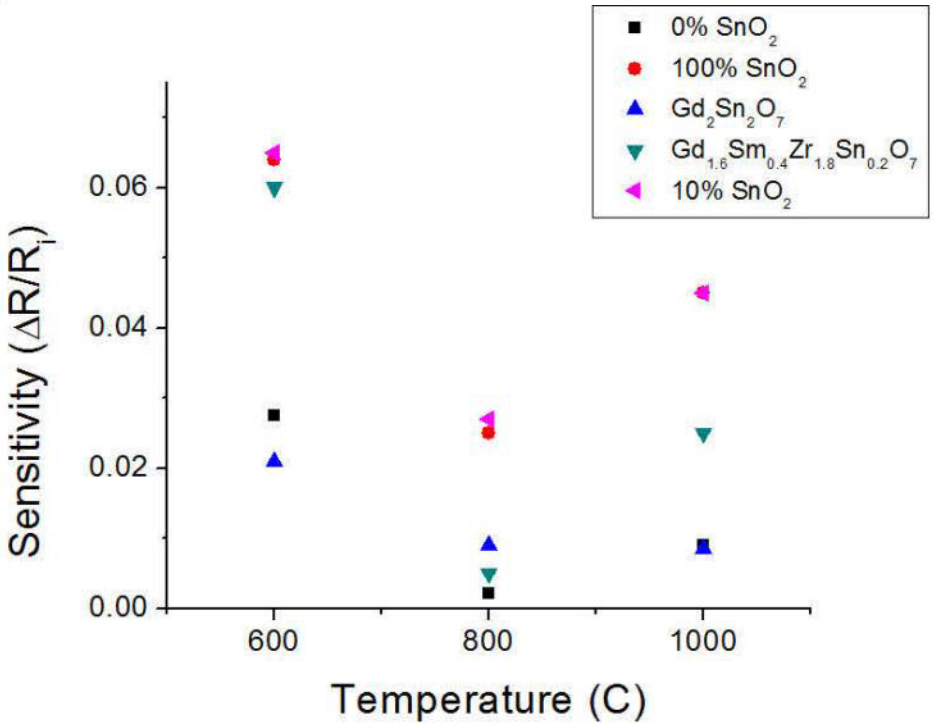

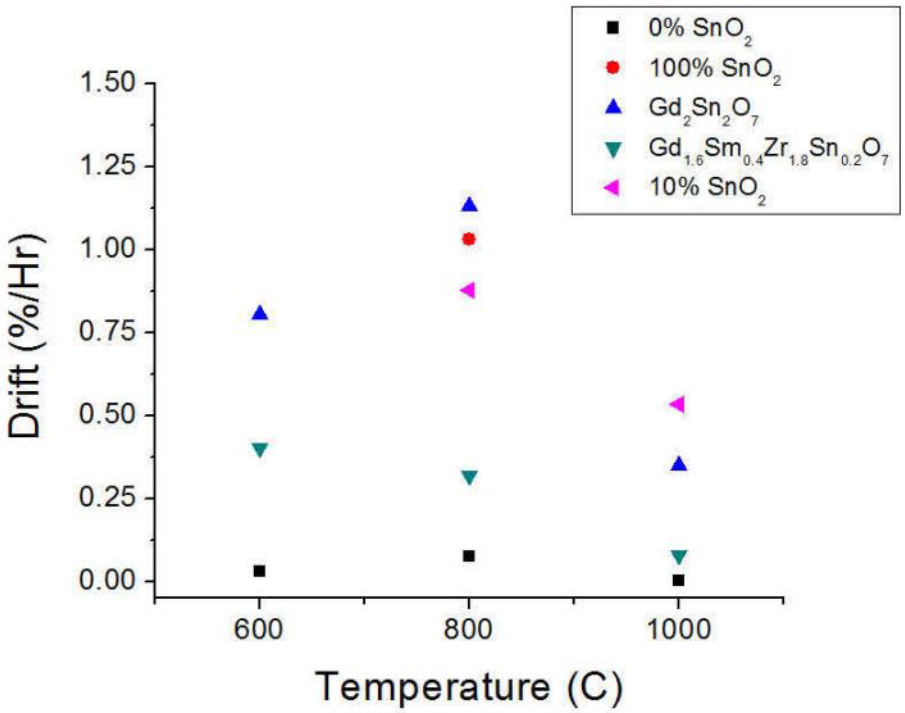

- Fully replacing Zr with Sn decreases sensitivity and increases drift
- Doping Zr site with 10% SnO_2 results in lower sensitivity than a 10% composite mixture but lower drift

Micro-Sensor Fabrication

1) **Pattern of high-temperature, stable, thin film electrodes:**
   - Platinum (Pt)-based sputtered electrodes.
   - Wet-etch or lift-off.
2) **Multiple techniques available to pattern sensing nanomaterial particulates in suspension/ink:**
   - LIGA
   - Stamping
   - Embossing
   - Micro-casting
   - Dip-pen nanolithography

Note: depositing nano-particulates, and not using typical CVD or PVD processes to deposit/pattern thin films.

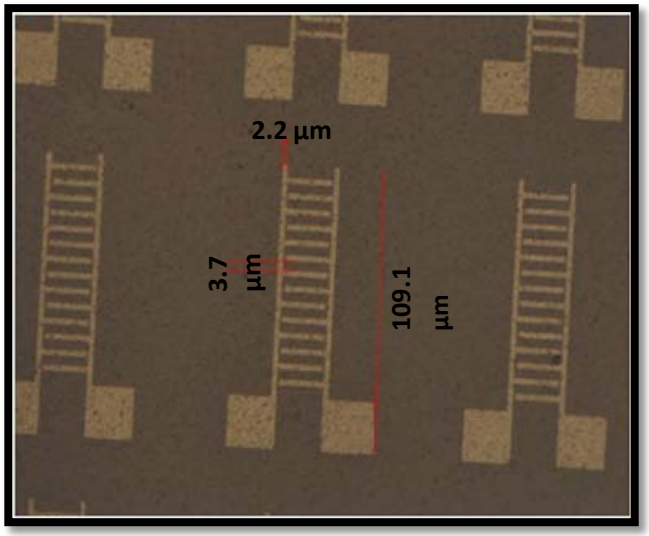

Patterning of Nano-Derived Micro-Sensors

Micro Molding - Nanomaterials

Lost-Mold Micro-casting

- SU8 is processed into molds onto substrate.
- Mold is removed during thermolysis and casted material bonds onto substrate.
- Feature thickness >20 µm can be demonstrated.
- Antolino et al. produced dense free-formed zirconia bars.

SU8 Micromolds

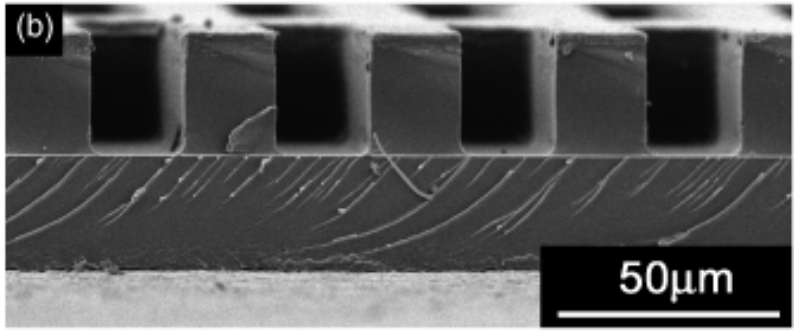

After Thermal Processing

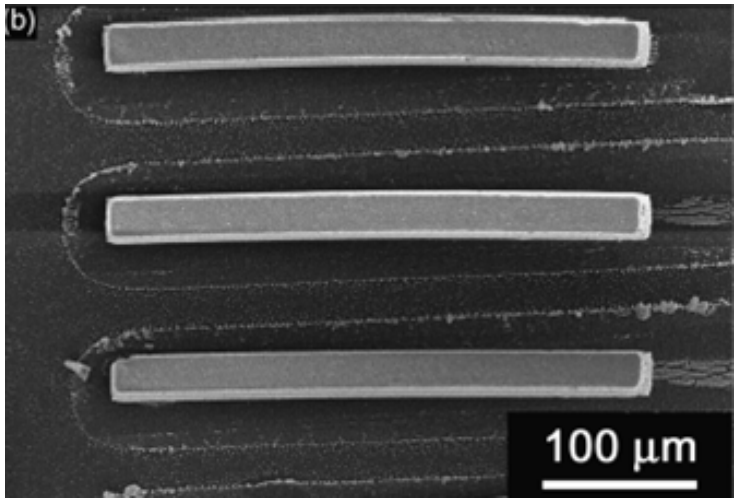

Antolino et al., Journal of American Ceramics Society, 92 (2009).

Micro-Casting Nanomaterials

- Negative Lithography for Micro-Molds
  - SU8-25 (Microchem)
    - From 20-90 µm depth depending on spin rate
  - OAI UV Flood Exposure System
  - SU8 developer
- Sensing Material is casted into mold
- Mold is burned off and material is sintered

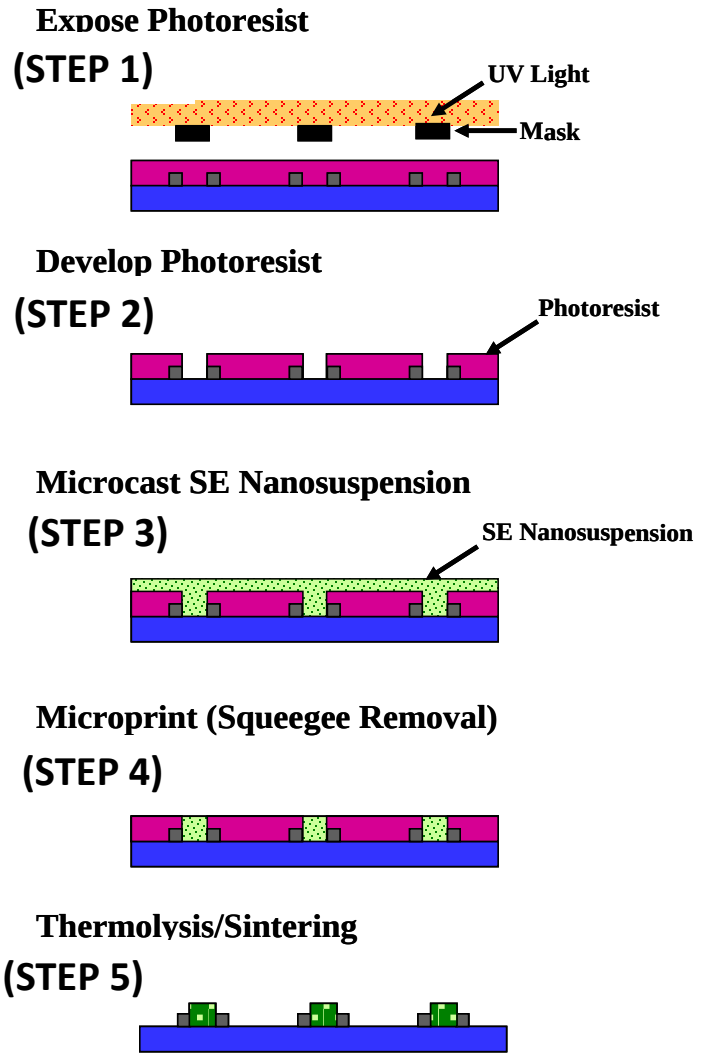

Micro-Casting

Stenciling with screenprinter

- Clean surface obtained
- Controlled pressure, squeegee speed
- Average viscosity of 300 poise at 8/s

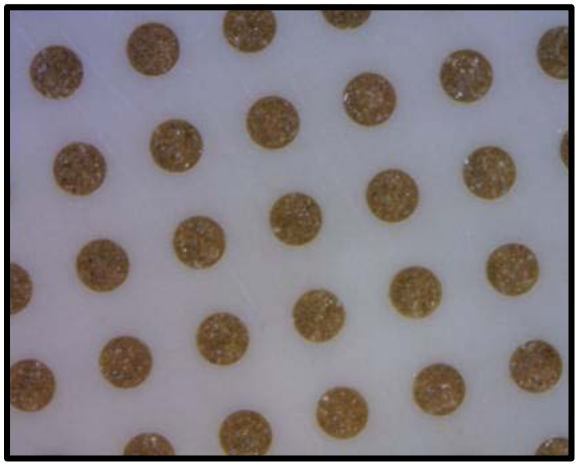

Micro-casting variables:

- Particle size
- Ink dispersion
- Rheology
- Mold geometry/dimensions
- Binder system

Micro-Casting - SEM

•Casted single layer on YSZ substrate

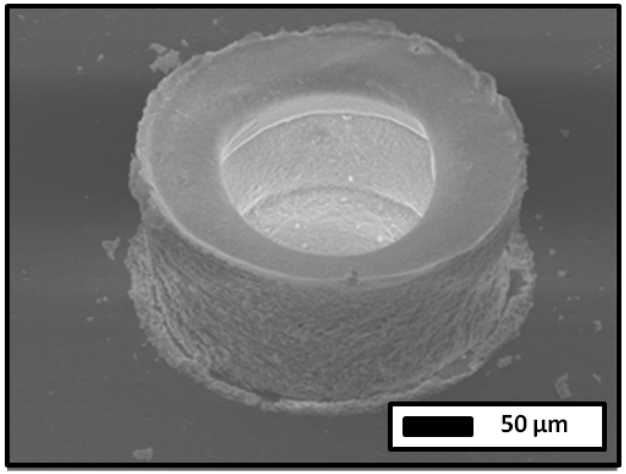

(a)

•Casted double layer on YSZ substrate

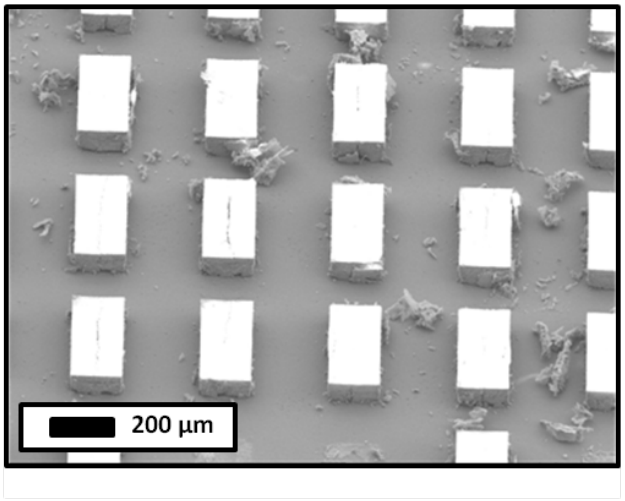

(b)

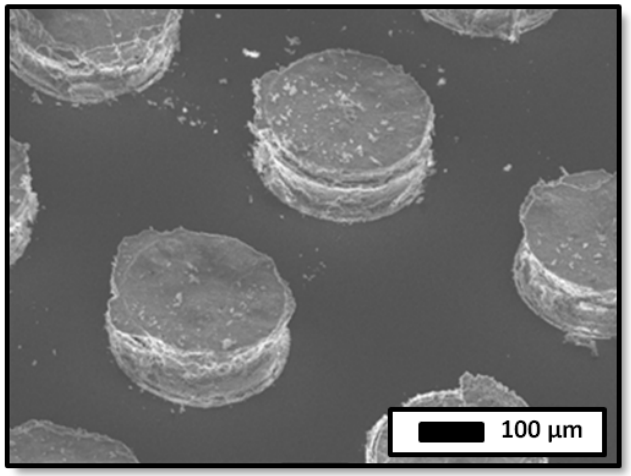

(c)

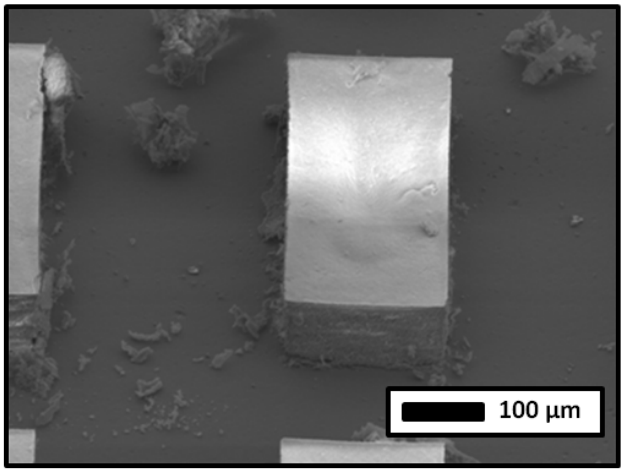

(d)

Micro-Casting– Aqueous Epoxy

- Aqueous epoxy system (Beckopax and Dicynex)
- Evidence of shrinkage
- Uniform particle packing
- Adequate shape retention.

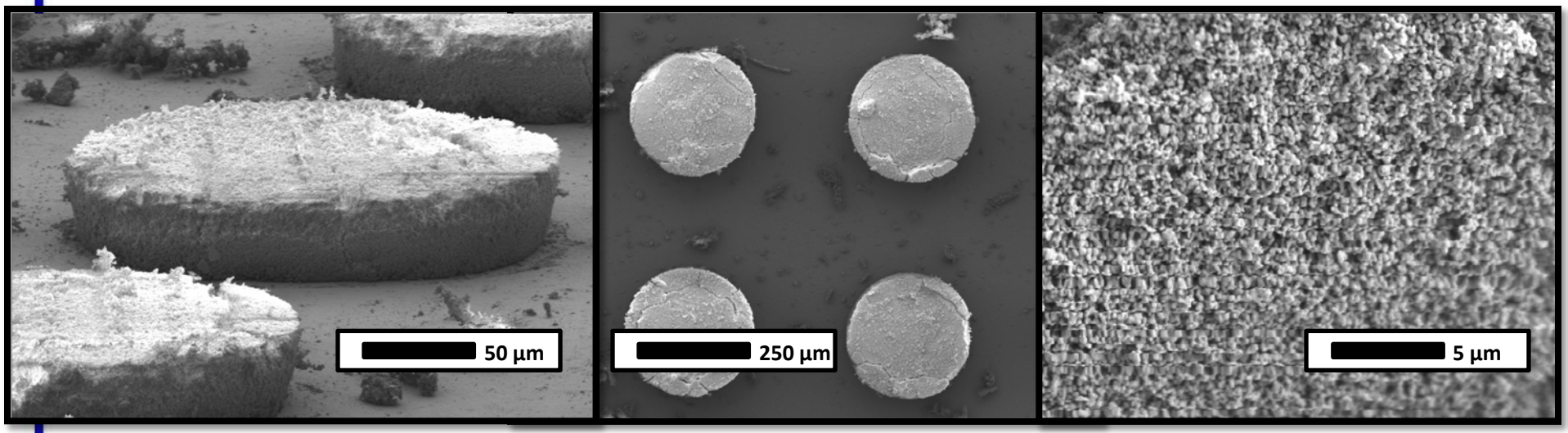

Micro-Casting – Aqueous Epoxy

Variation of solids loading and sintering temperature

- Compared 12%, 20%, and 30 vol% solids loading in water-based epoxy system
  - Single casting
  - Noticed increased stability with solids loading (left)
- Sintered at 1200˚C and 1300˚C
  - Significant shrinkage increase with temperature increase (right)

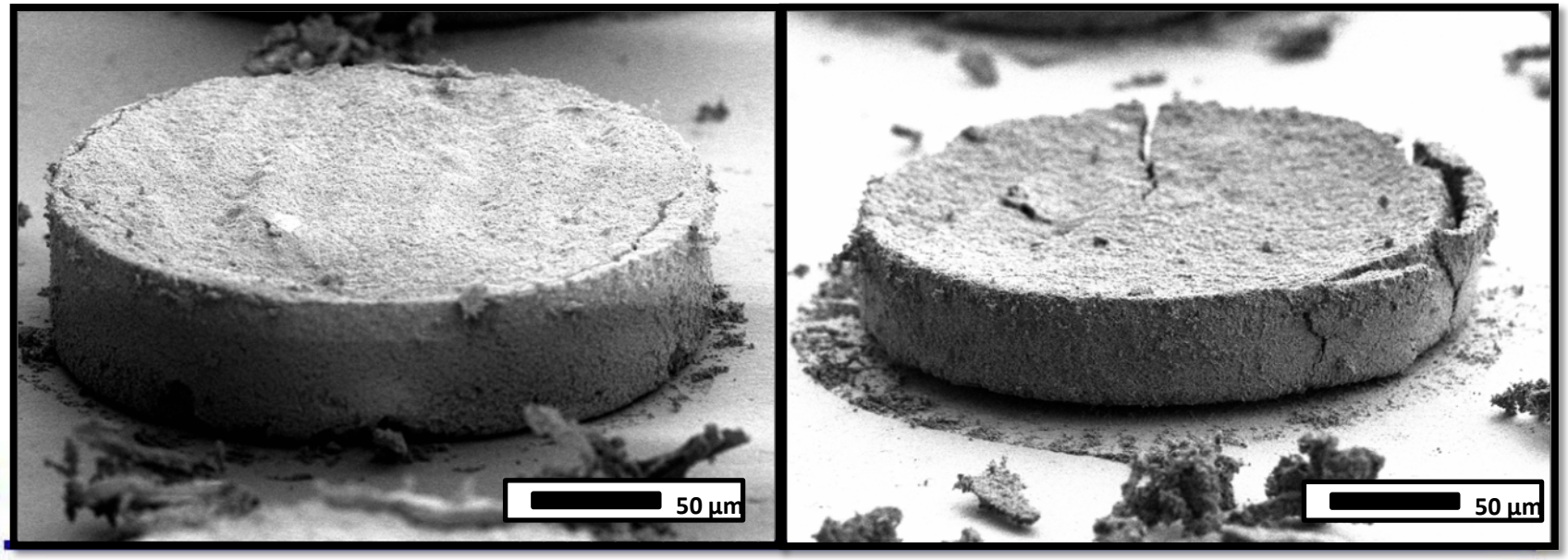

Wetting Measurements (Aqueous Epoxy)

Substrate	12 vol%	20 vol%	30 vol%
Alumina	55.792 θ 	52.640 θ 	
YSZ	46.975 θ 	50.868 θ 	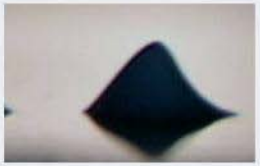
SU-8	61.721 θ 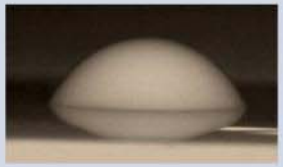	61.587 θ 	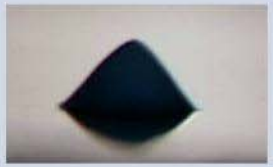

- Critical particle loading is reached, capillary force pulls liquid in and fights surface tension.
- Therefore, there is a limitation on particle loading due to particle interaction.

Micro-casting –

Aqueous Acrylate and Terpineol-based Systems

- SEM revealed water based (MAM:MBAM) gel casting did not cup but collapsed due to air bubble (Left)
- SU8 seems to attract terpineol-based ink suspention forming hollow cylinders (Right)

MAM:MBAM

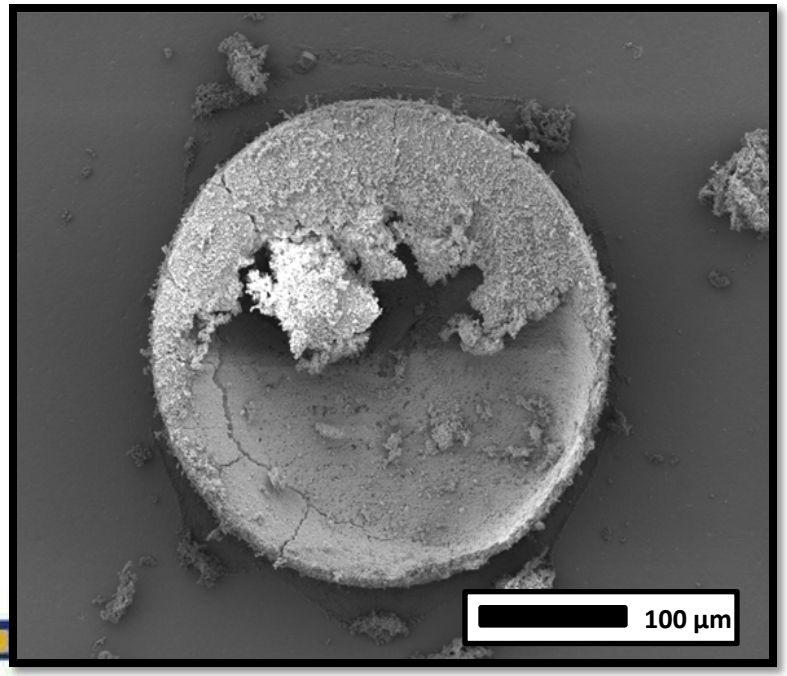

Terpineol-Ethyl cellulose

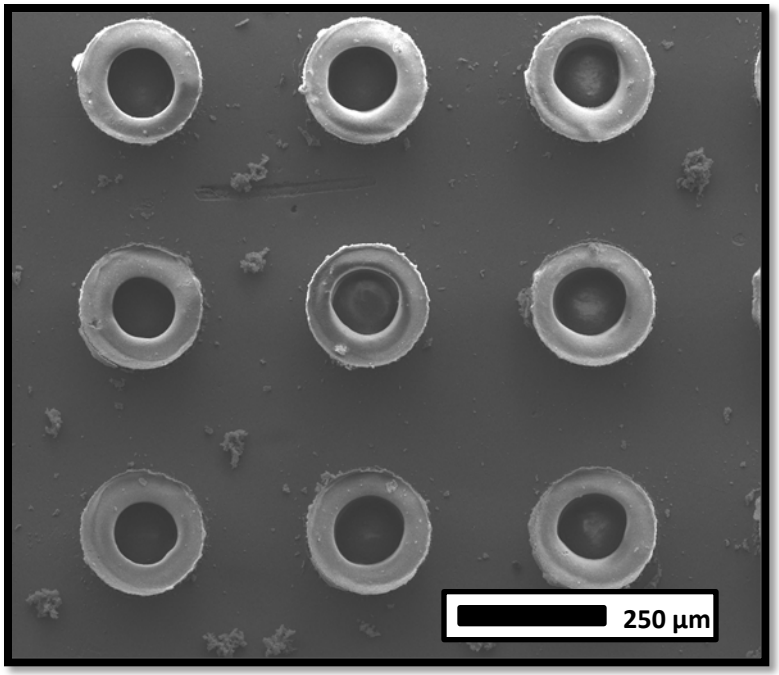

Wetting Measurements (Terpineol-based System)

	0 wt%	5 vol%	10 vol%	15 vol%	25 vol%
Alumina (θ)	19.341	18.670	27.001	30.352	48.720
YSZ (θ)	19.269	18.478	23.199	25.537	44.361
SU-8 (θ)	20.732	19.646	22.576	25.904	46.425

.

- Binder system wets SU-8 mold very well.
- Wicking of solvent into SU-8 results in well-packed molded features (similar to slip-casting).

Micro-Patterning Techniques

Dip Pen Nanolithography (DPN)

- Direct drawing delivers multiple materials onto a single substrate.
- Typically used to deposit organic material (DNA, cells, peptides, polymers).

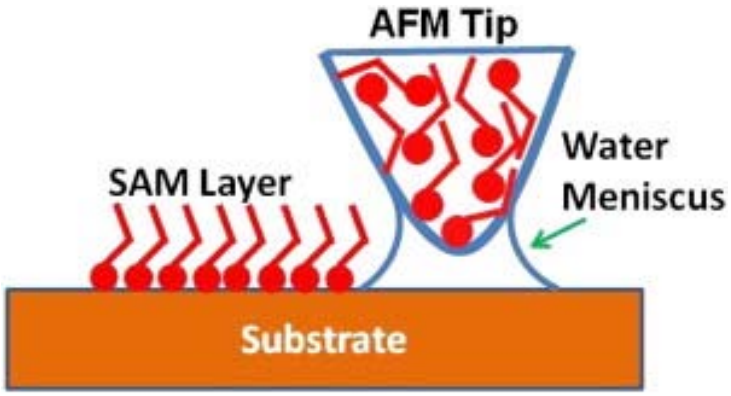

Mirken group (Northwestern Univ.) work with AFM writing in 1999.

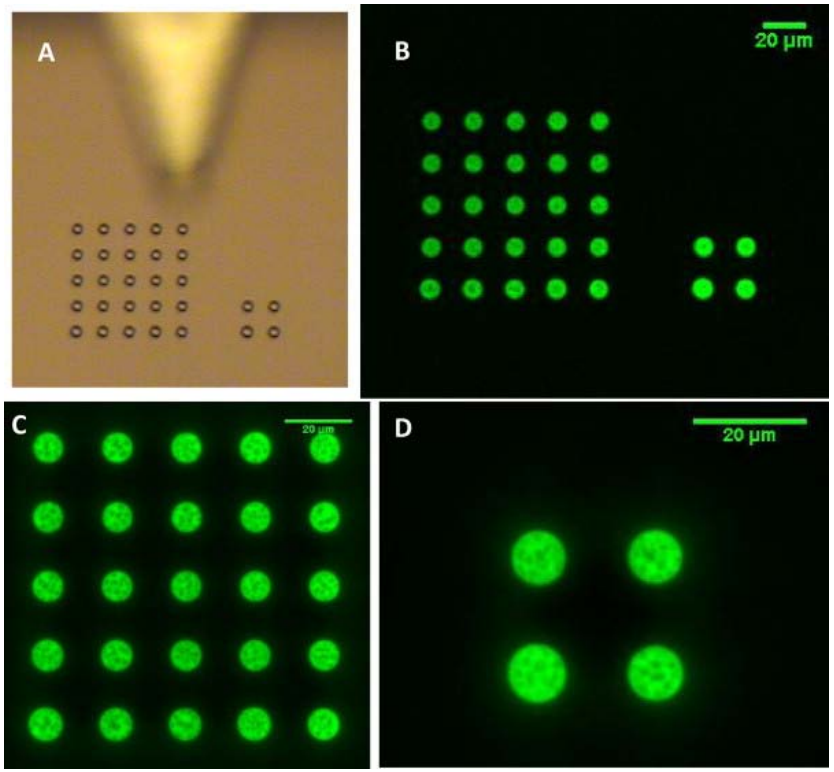

Thompson et al., Biosensors and Bioelectronics, 26 (2011).

Agarwal et al., Thin Solid Films, 519(2010).

DPN on Untreated Substrate

	Cu Ink #1		Cu Ink #2	
	Wet	Dry	Wet	Dry
Glass	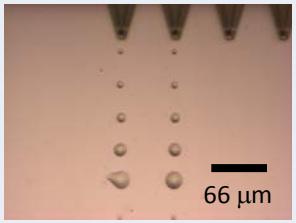	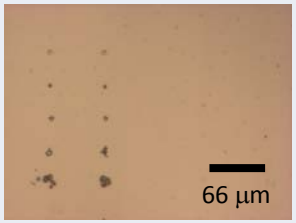	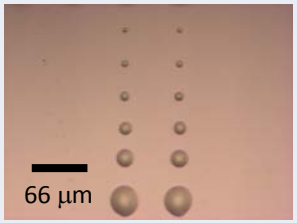	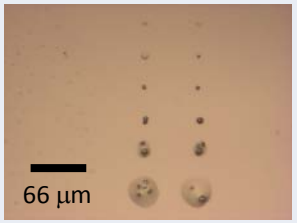
Alumina	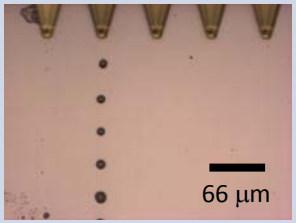	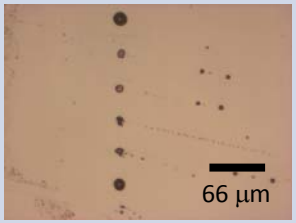	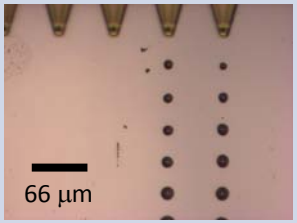	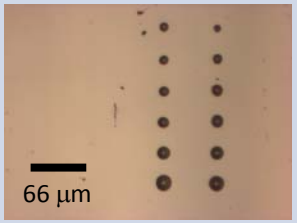

- Ink shows **θ≈35°** on both substrates.
- Uniform size and shape dots (5-10 μm) possible on alumina substrate.
- Ink #2 dots on alumina substrate retain shape through drying.
- Direct-writing of continuous line not possible on neither substrates **(contact angle too high, >25° for line drawing).**

Electroded Ceramic Alumina Substrates

	Substrate	Pattern with Ink #2
No coating	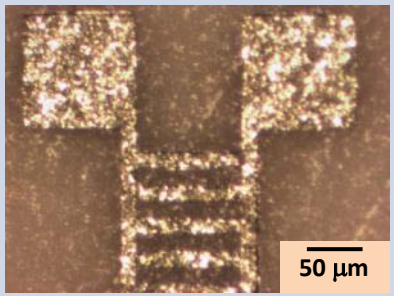	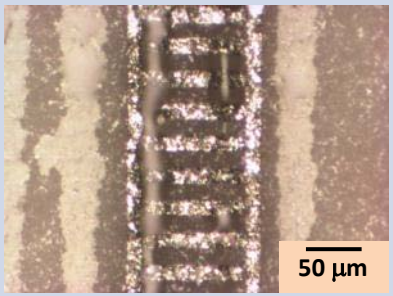
CTAB coating	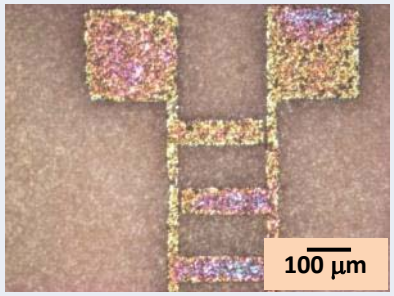	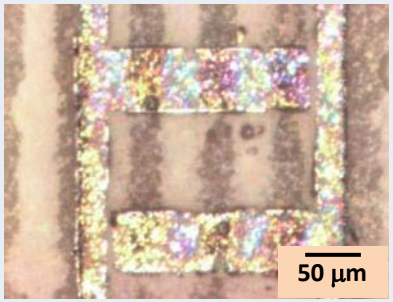

- Patterning on ceramic (polycrystalline) substrate with metallic electrodes.
- Difficult due to difference in wetting characteristics of each grain and metal vs. ceramic.

- Cu ink pattern on a substrate ***without a coating*** shows the ink **stumbling over the metallic/ceramic interchanges.**

- CTAB coating provides a single chemistry surface over the IDEs on multigrain ceramic substrate.

- CTAB coating enables patterning Cu sol-gel inks.

Fabrication of Stable Micro-IDEs

Background: Electrodes for Electrochemical Sensing Applications

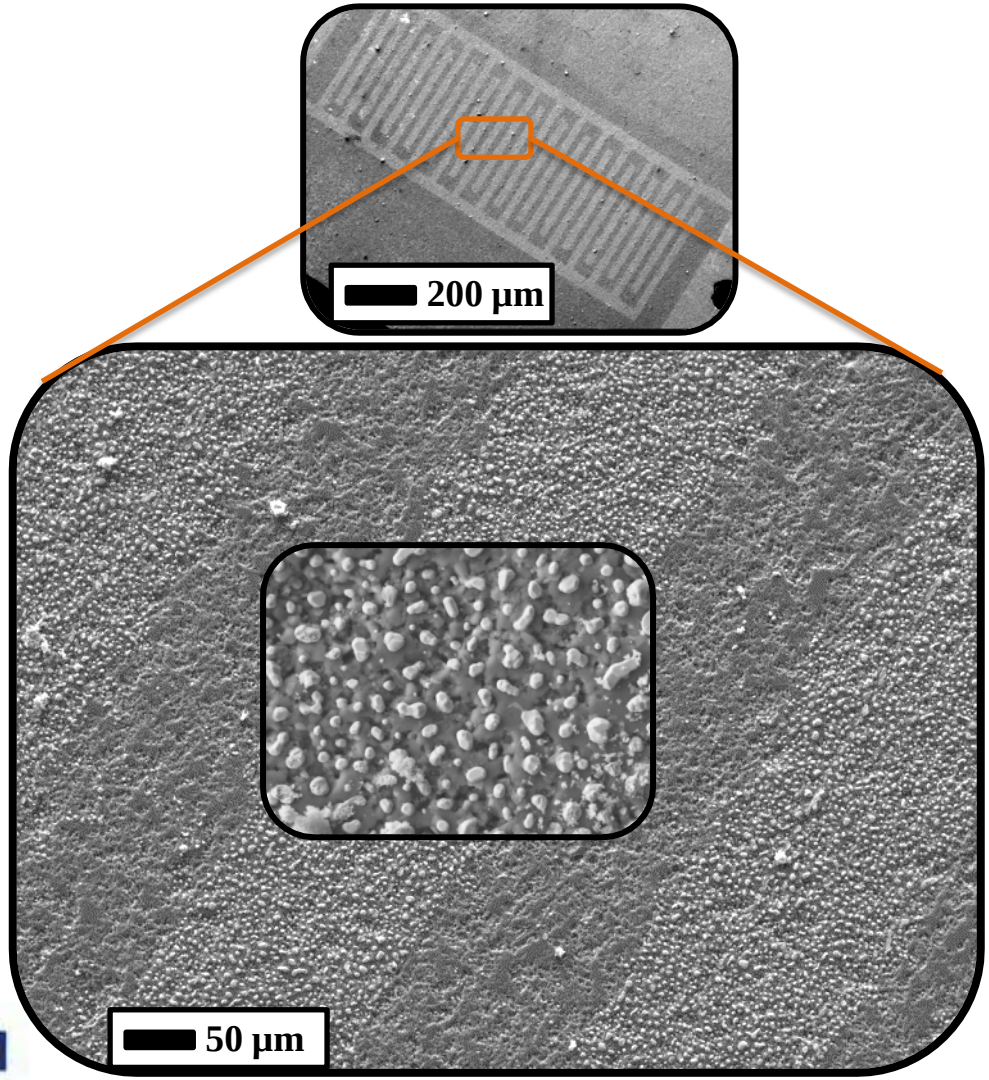

Current sensor technology is limited to operate at low temperature due to

- Sensing material composition
- Processing
- **Incapable electrodes**

Breaks Apart !!!

Solution In Order to Hinder Degradation of the Pt Thin Film

- **Using intermediate layer i.e. adhesion layer so-called glue layer.**

Surface tension

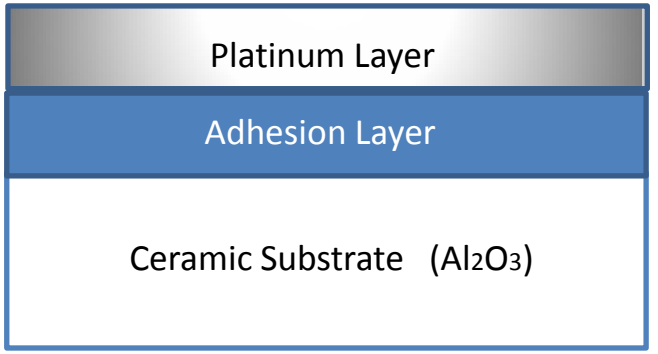

Combat

- **Using second phase precipitation.**

Coarsening

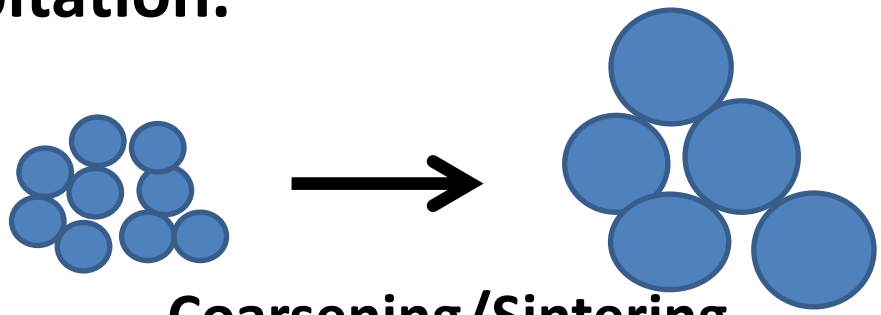

Coarsening/Sintering

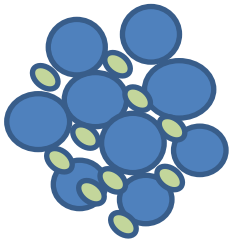

Grain Boundary Pinning Hinders Coarsening.

: Pt grain

: Second phase grain

Objectives

1) High-temperature degradation of Pt thin films deposited onto alumina substrates.
2) Effect of Ti, Ta, Zr, and Hf adhesion layers on hillock formation and coarsening/sintering.
3) Zener-pinning effect and combination with suitable adhesion layer.

Experimental Procedure: Processing

Deposition method:

- DC Magnetron Sputtering deposition on Al_2O_3 wafer
- Alumina wafer characteristics, R_a=34 nm

- **Deposition parameters:**
  - Primary gas pressure (Argon): 60 mTorr
  - Deposition Power : 100 watt
  - Deposition temperature: 200°C

- **Thicknesses regardless of coating type:**
  - Pt=425 nm
  - Adhesion layer=35 nm

Adhesion layer (35 nm)	**Identification of the coating architecture**
Platinum	Pure Pt
BILAYER COATING ARCHITECTURES	
Titanium	Ti+Pt
Tantalum	Ta+Pt
Zirconium	Zr+Pt
Hafnium	Hf+Pt
MULTILAYER COATING ARCHITECTURES	
Zirconium	L-Zr+Pt
Hafnium	Hf+L-Zr+Pt

Experimental Procedure: Characterizations

High-temperature stability testing:

- Isothermal annealing in N_2 to 800-1200°C for 1-48 hours.
- SEM and XPS completed on annealed sample surface.

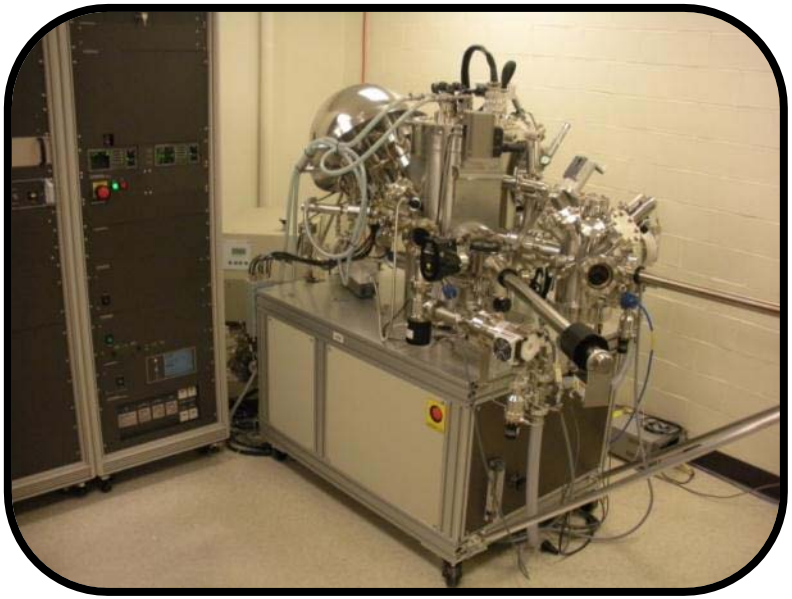

Electrical resistivity testing:

- Van der Pauw method

[Philips Research Reports 13 1-9, 1952]

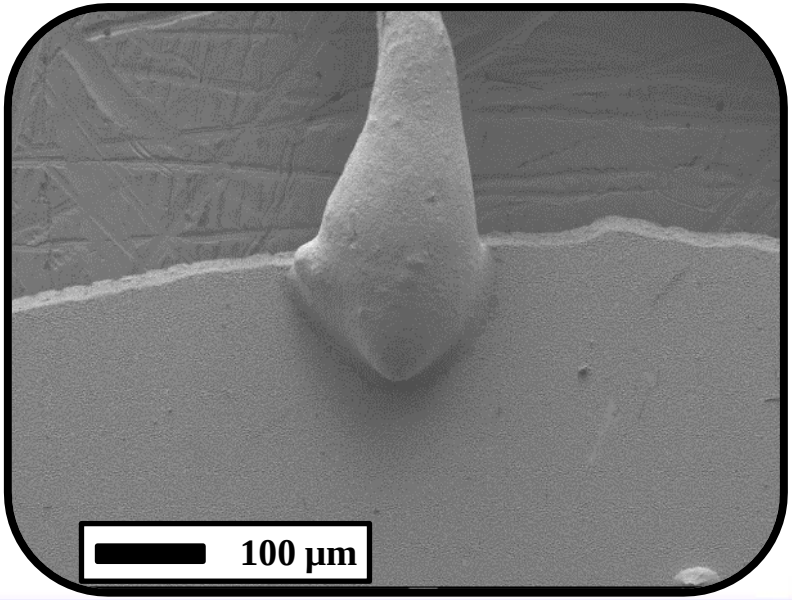

Definition of Coating Architectures

Schematic Representations

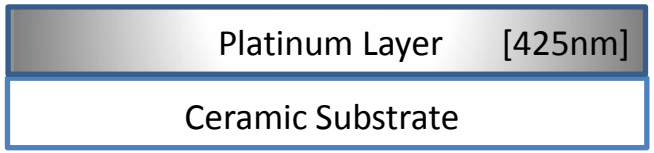

Pure Pt

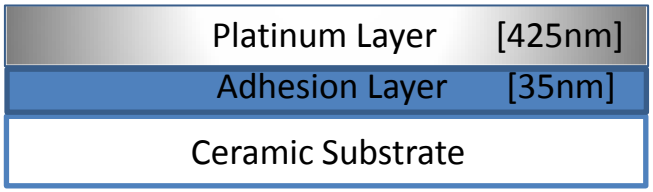

BILAYER COATING ARCHITECTURES	
Titanium	Ti+Pt
Tantalum	Ta+Pt
Zirconium	Zr+Pt
Hafnium	Hf+Pt

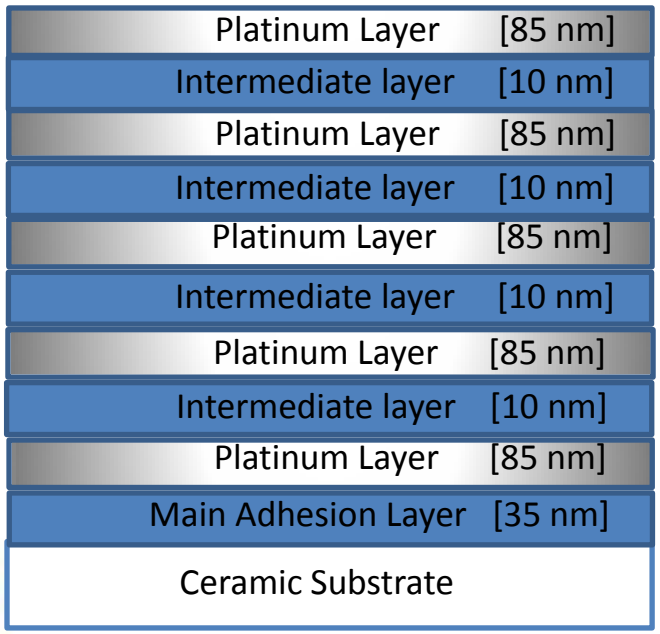

MULTILAYER COATING ARCHITECTURES	
Zirconium	L-Zr+Pt
Hafnium	Hf+L-Zr+Pt

Pure Pt on Alumina

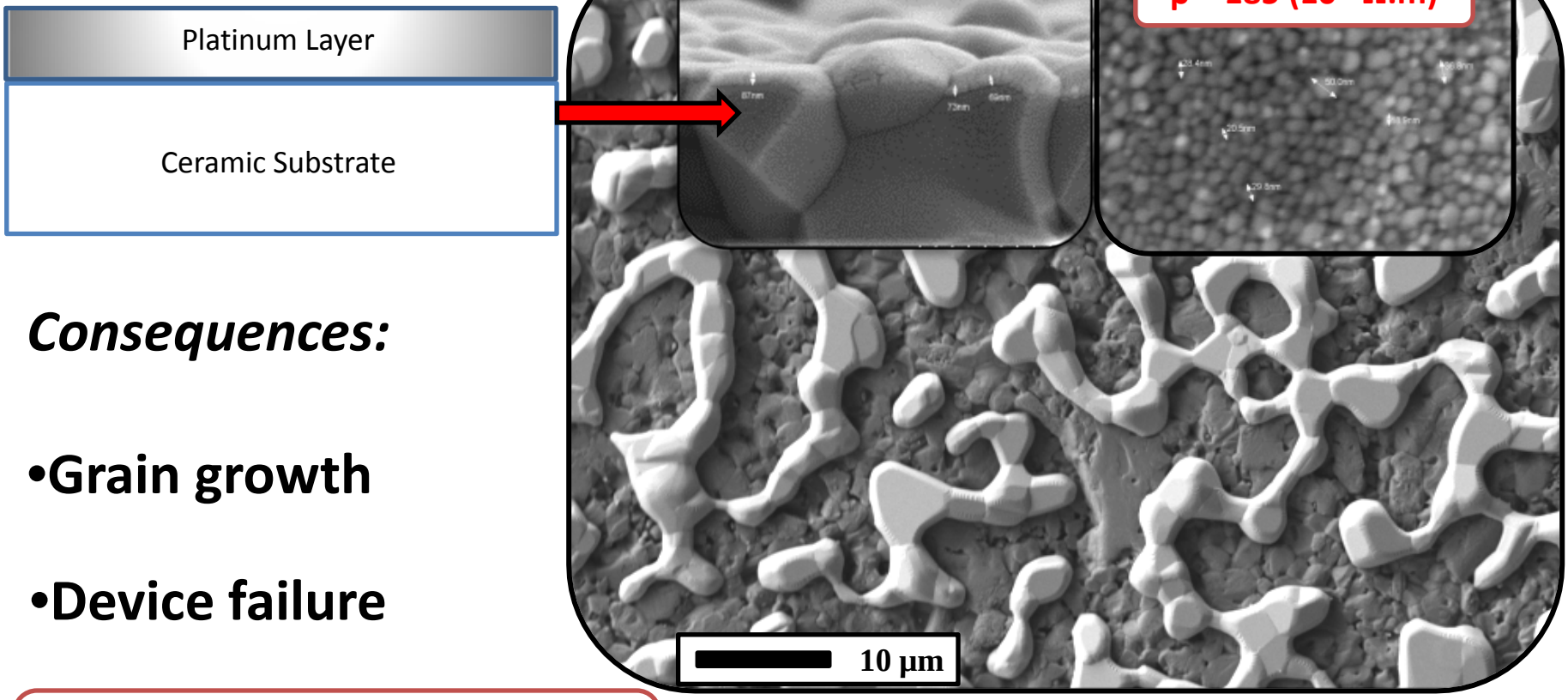

Consequences:

- **Grain growth**
- **Device failure**

ρ = ∞ (10^{-9} Ω.m)

Pt on ceramic without adhesion layer, after 1200°C 1 h inert atmosphere annealing

Bulk resistivity of Pt, ρ = 106 (10^{-9} Ω.m)

Bilayer Coatings; Ti+Pt and Ta+Pt

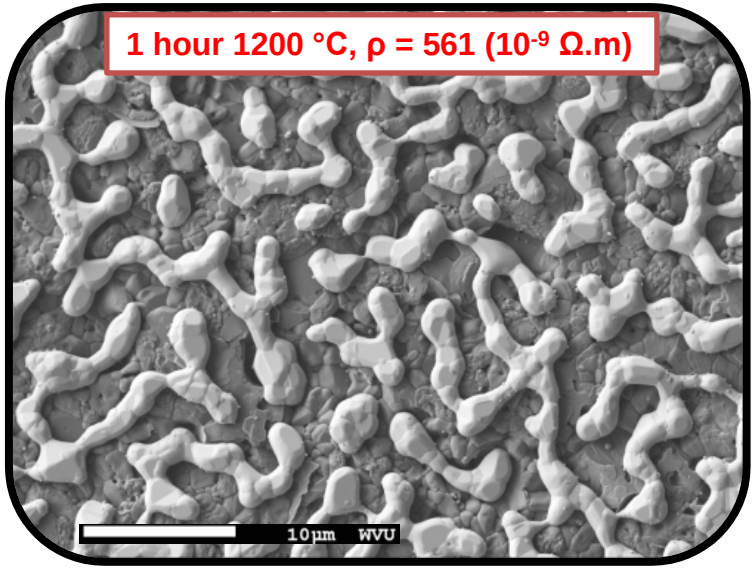

XPS of Ti+Pt film surface after 800 °C

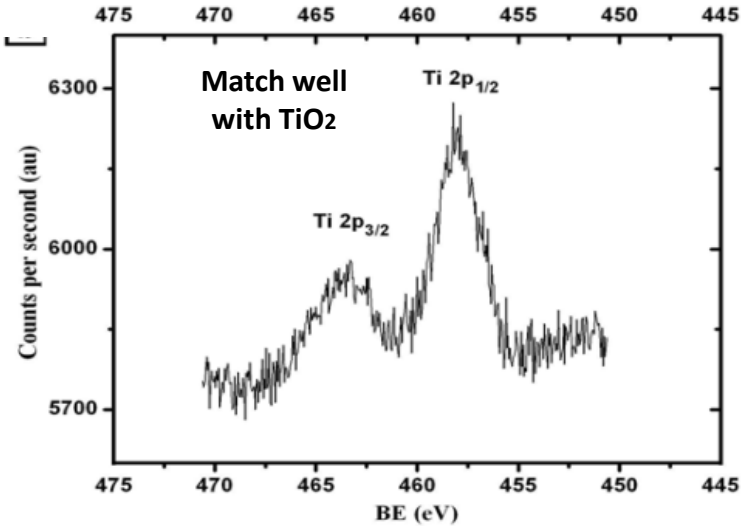

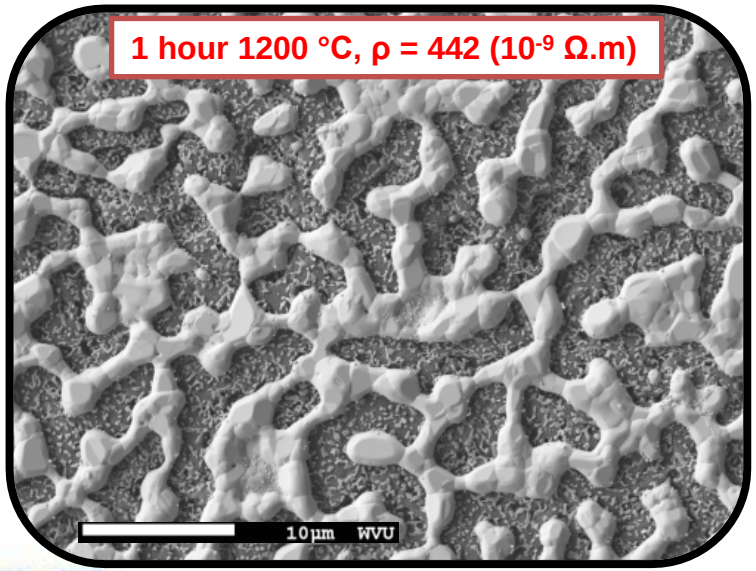

LOST OF ADHESION LAYER

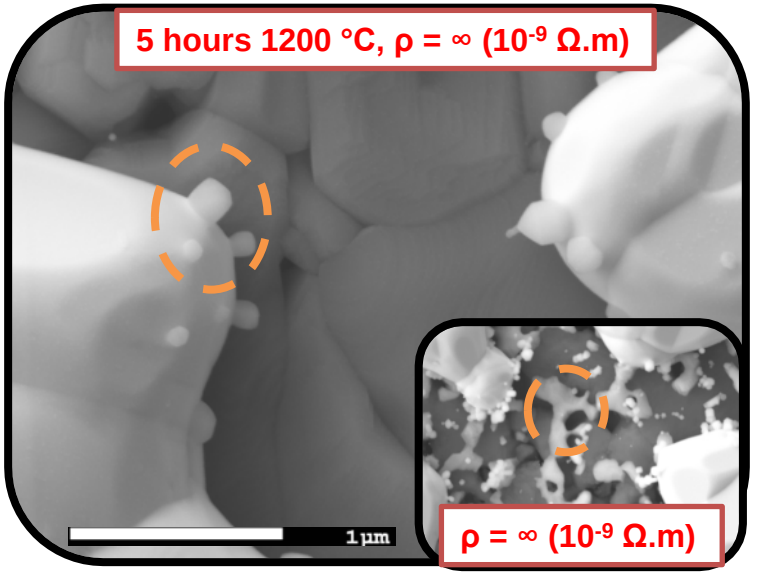

Bilayer Coatings; Zr+Pt

A few researchers worked with Zr as an adhesion layer ;

T. Maeder, *Jpn. J. Appl. Phys.* 1993.
C. C. Mardare, *Appl. Surf. Sci., 2005.*
M.P Cunha, *Ultrasonics Symposium, IEEE .,2007.*

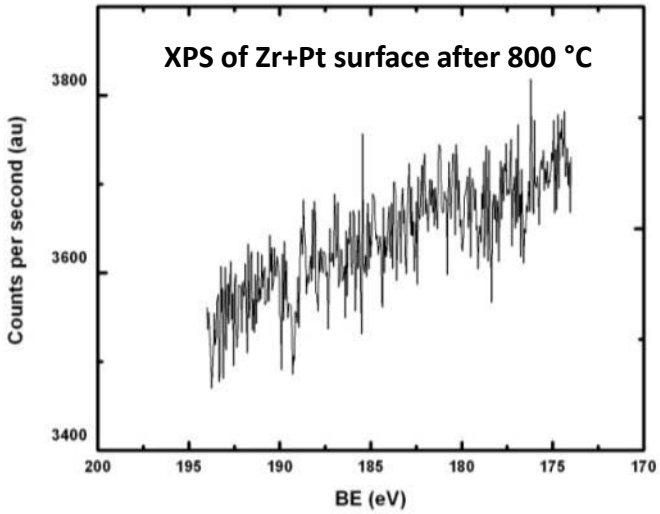

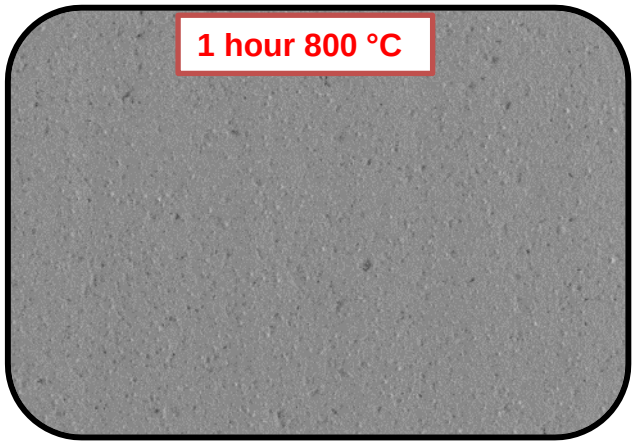

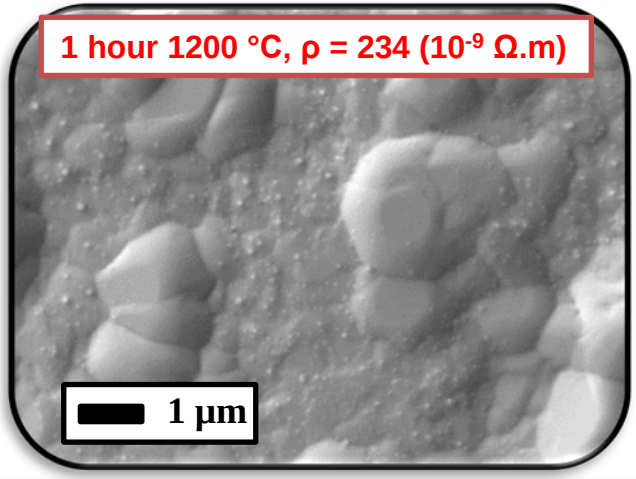

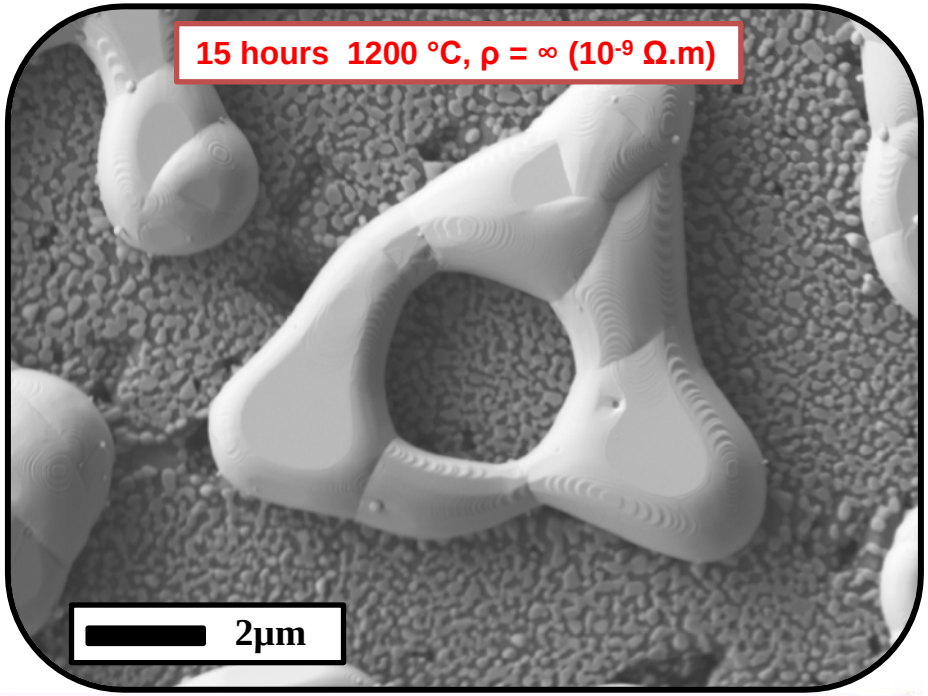

Bilayer Coatings; Hf+Pt

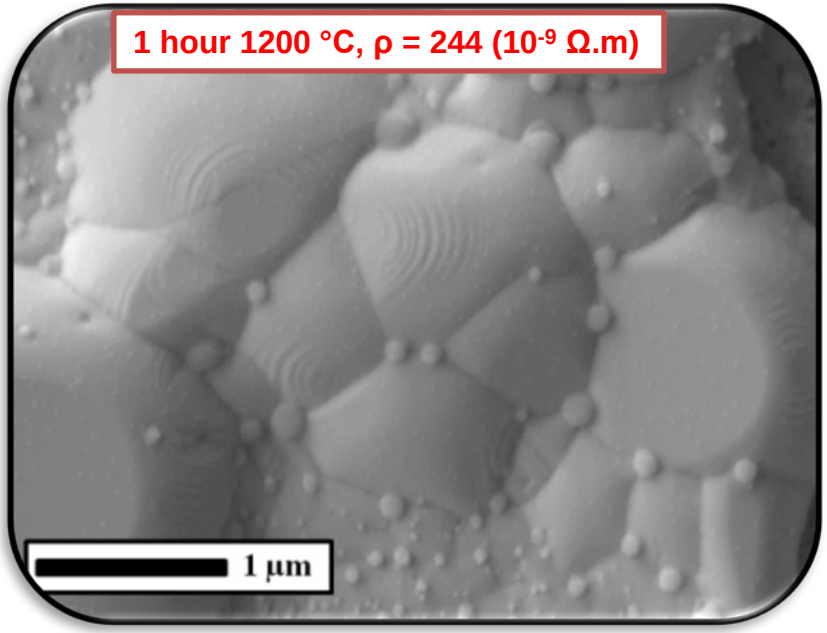

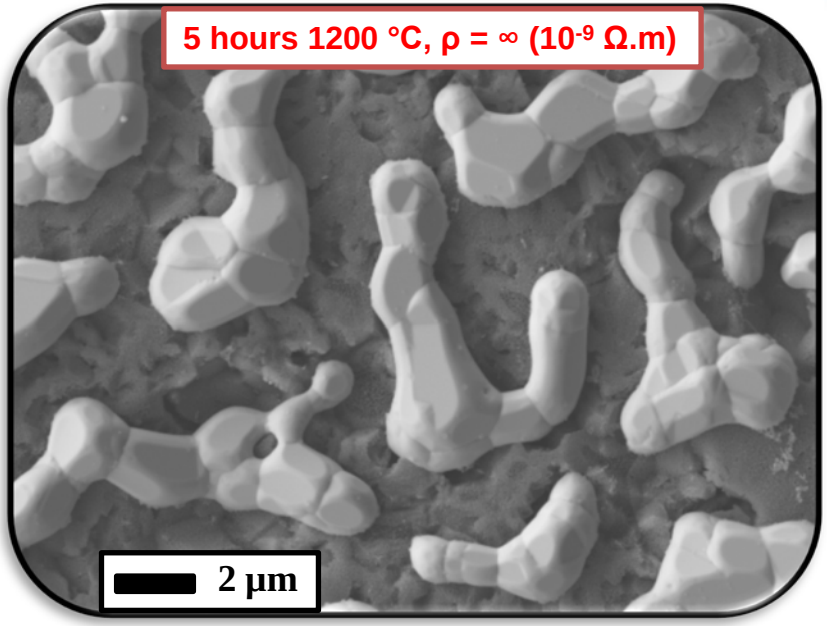

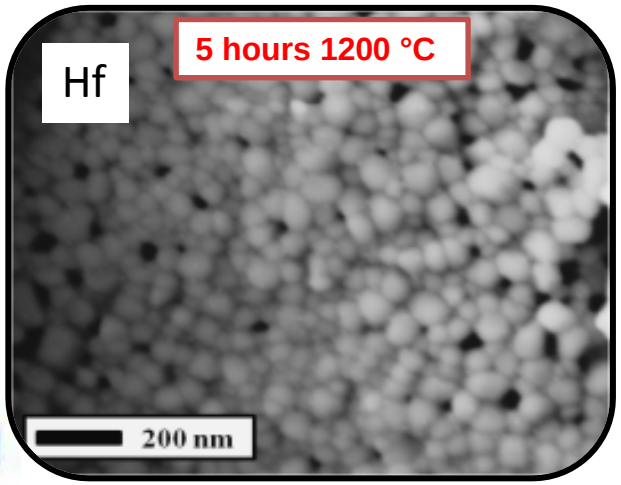

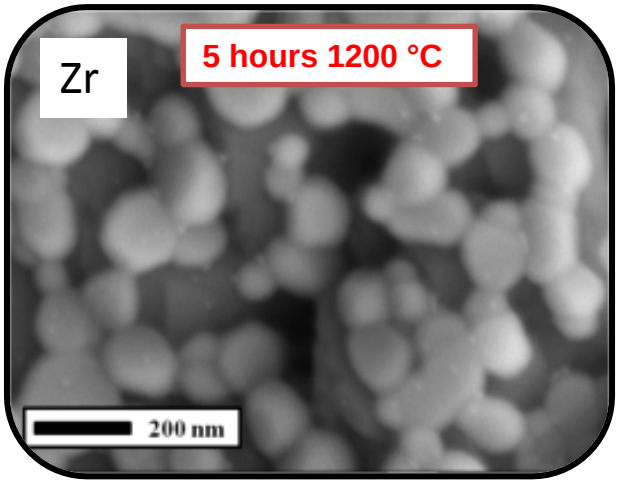

- Slow diffusion of Hf in Pt.
- Improved durability in adhesion layer.

Bilayer Coatings; Diffusion Behaviors of Hf and Zr

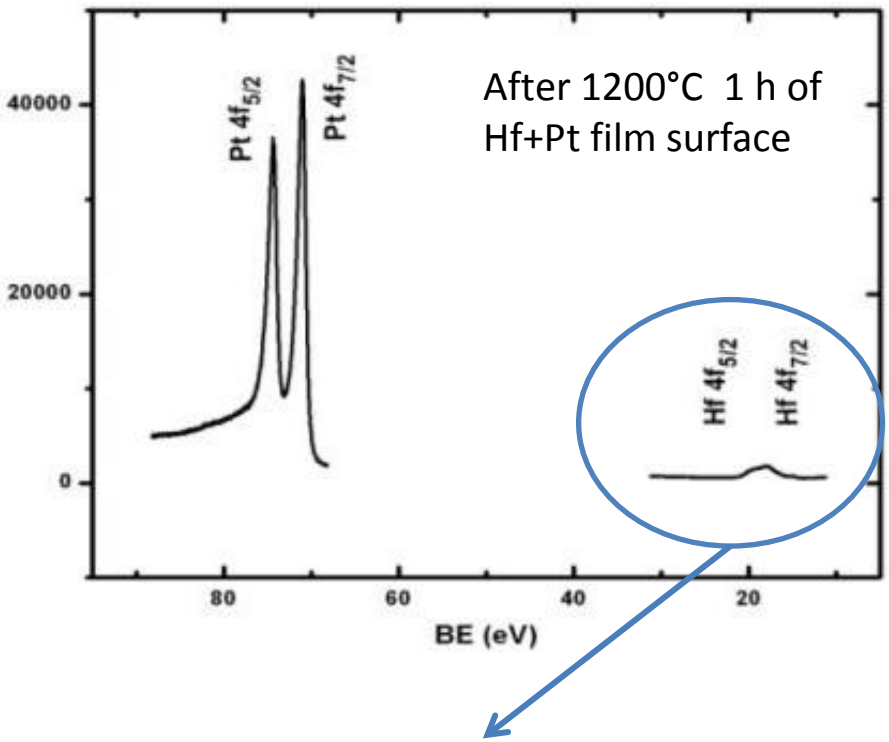

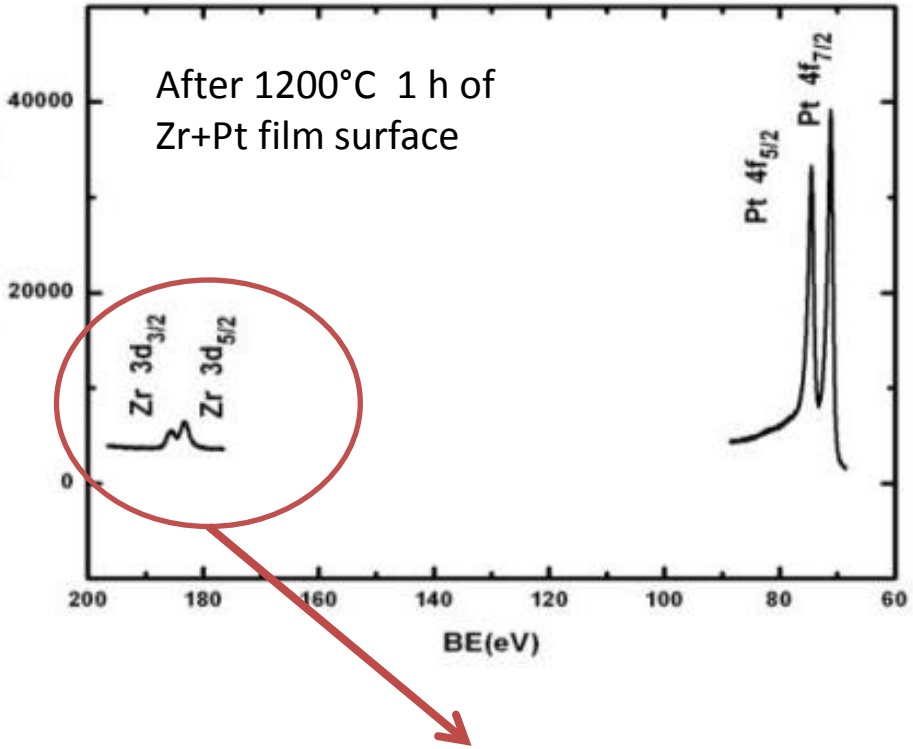

Hf 4.5% of the Hf+Pt film

Zr 13.5% of the Zr+Pt film

Summary of Adhesion Layer Study

Adhesion layer (35 nm)	Identification of the coating architecture
Platinum (not reliable >700 °C)	Pure Pt
Titanium (moves all the way up)	Ti+Pt
Tantalum (better but not sufficient)	Ta+Pt
Zirconium (for intermediate layers)	Zr+Pt
Hafnium (very stabile adhesion layer)	Hf+Pt
Layer by Layer Zirconium	L-Zr+Pt
Hafnium based Layer by Layer Zirconium	Hf+L-Zr+Pt

Objective 1: Effect of Ti, Ta, Zr, and Hf adhesion layers on hillock formation and coarsening

Conclusions:

- All show hillock formation and diffusion
- Zr adequate for adhesion layer
- Hf shows best stability

NEXT STEP: Multilayer coatings in order to hinder coarsening

Multilayer Coatings; L-Zr+Pt

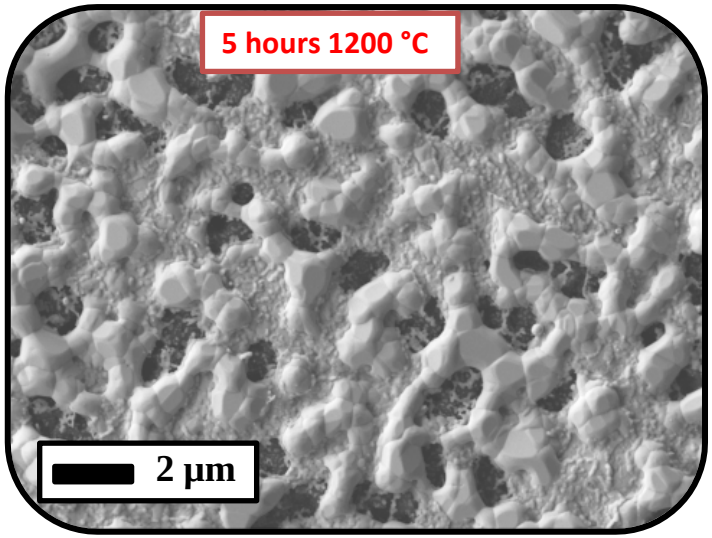

Platinum Layer	[85 nm]
Intermediate layer	[10 nm]
Platinum Layer	[85 nm]
Intermediate layer	[10 nm]
Platinum Layer	[85 nm]
Intermediate layer	[10 nm]
Platinum Layer	[85 nm]
Intermediate layer	[10 nm]
Platinum Layer	[85 nm]
Main Adhesion Layer	[35 nm]
Ceramic Substrate	

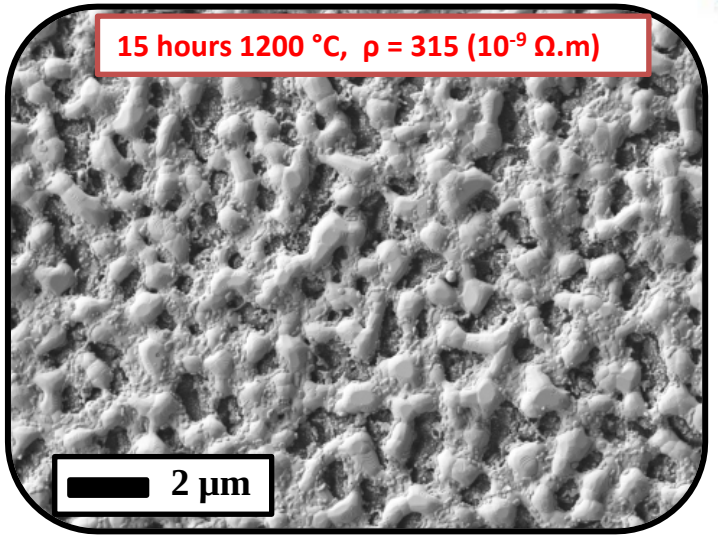

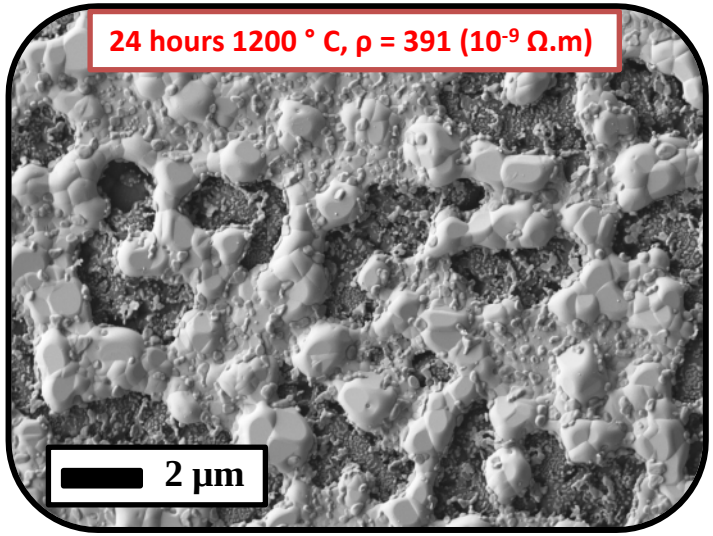

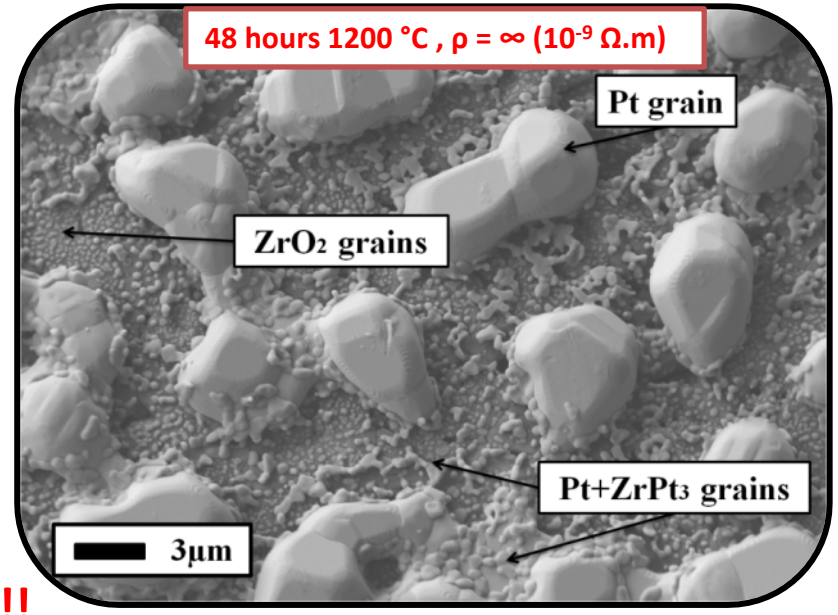

Extended high temperature service life !!!

Multilayer Coatings; Hf+L-Zr+Pt

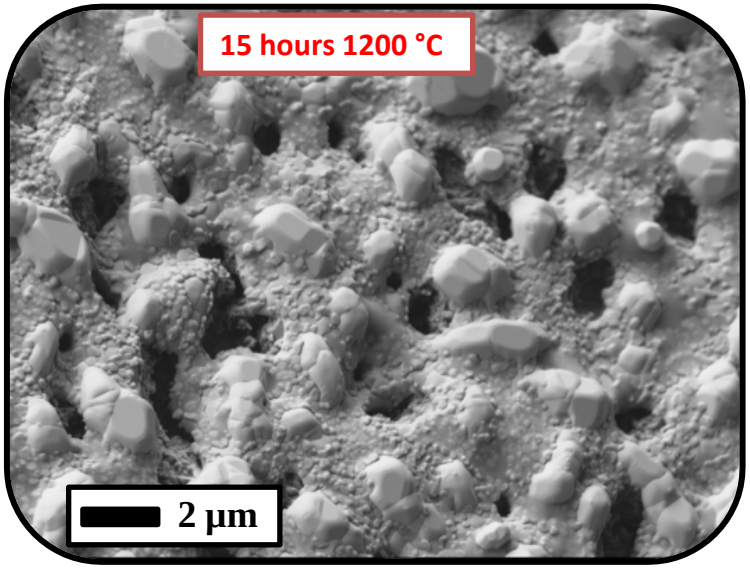

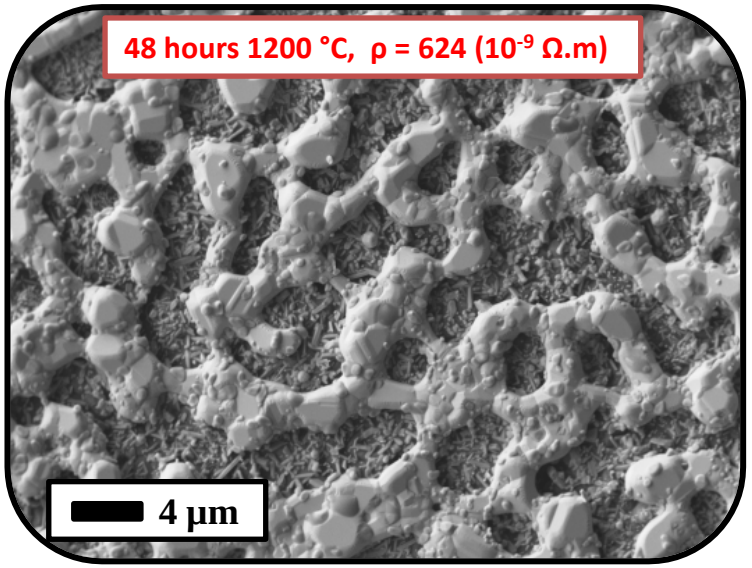

- **Better performance.**
- **Durable adhesion layer.**
- **The most stabile intermetallic, $HfPt_3$.**

[P. Ficalora *et al.* Department of the Navy Mar. 1971]

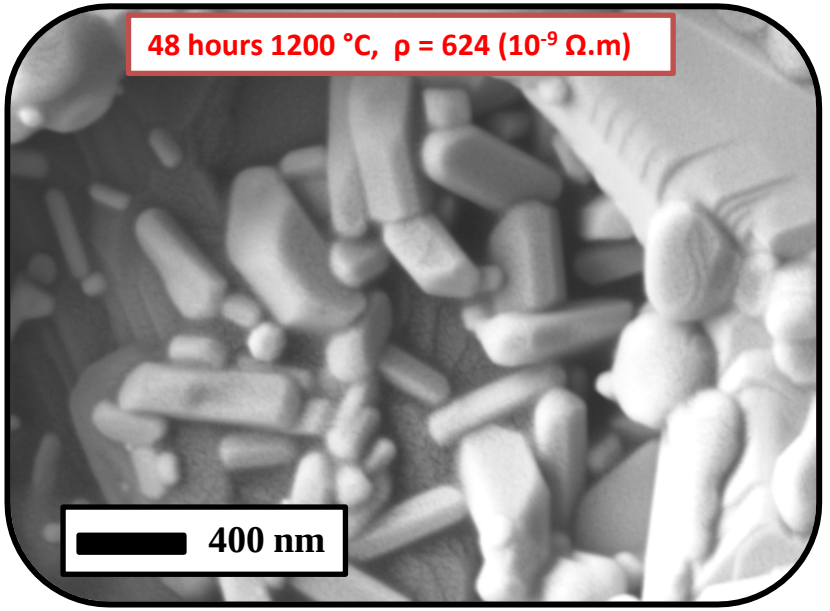

Multilayer Coatings; Hf+L-Zr+Pt

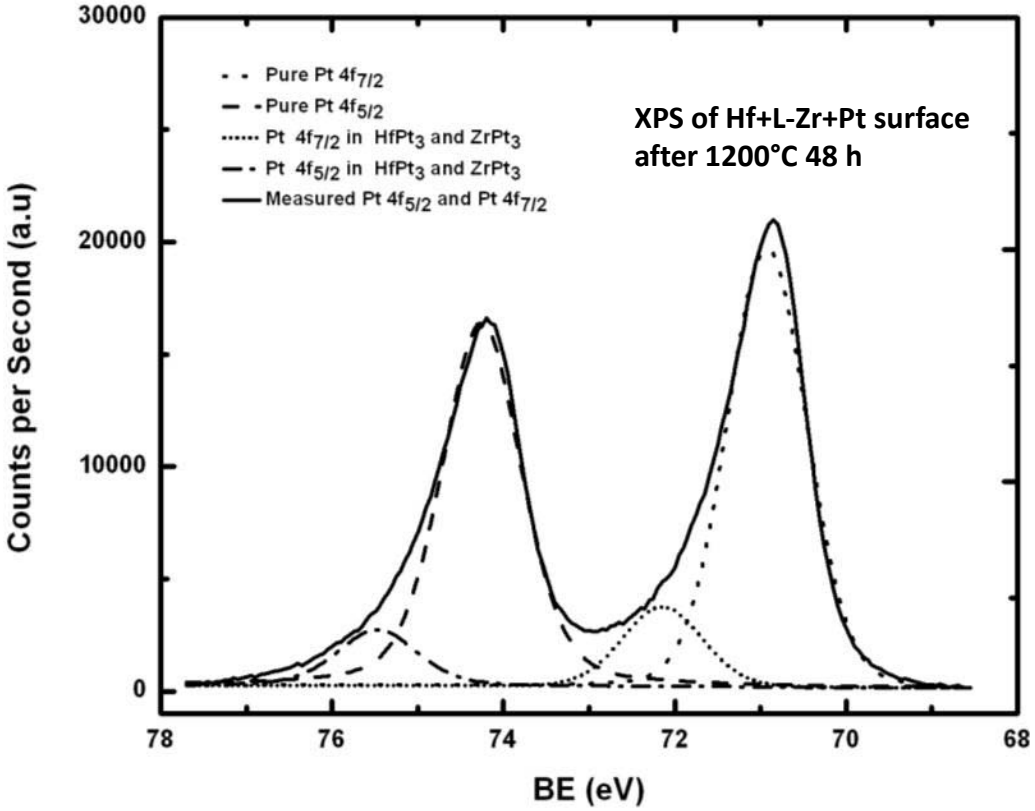

XPS Detailed Spectrum of Pt 4f Doublet

- **Broadening due to intermetallic formation of $HfPt_3$ and $ZrPt_3$.**
- **(~0.67%) higher than the value found in the literature work for $HfPt_3$.**

[Wertheim *et al. Phys. Rev. B. 1989]*

Summary: Improvement

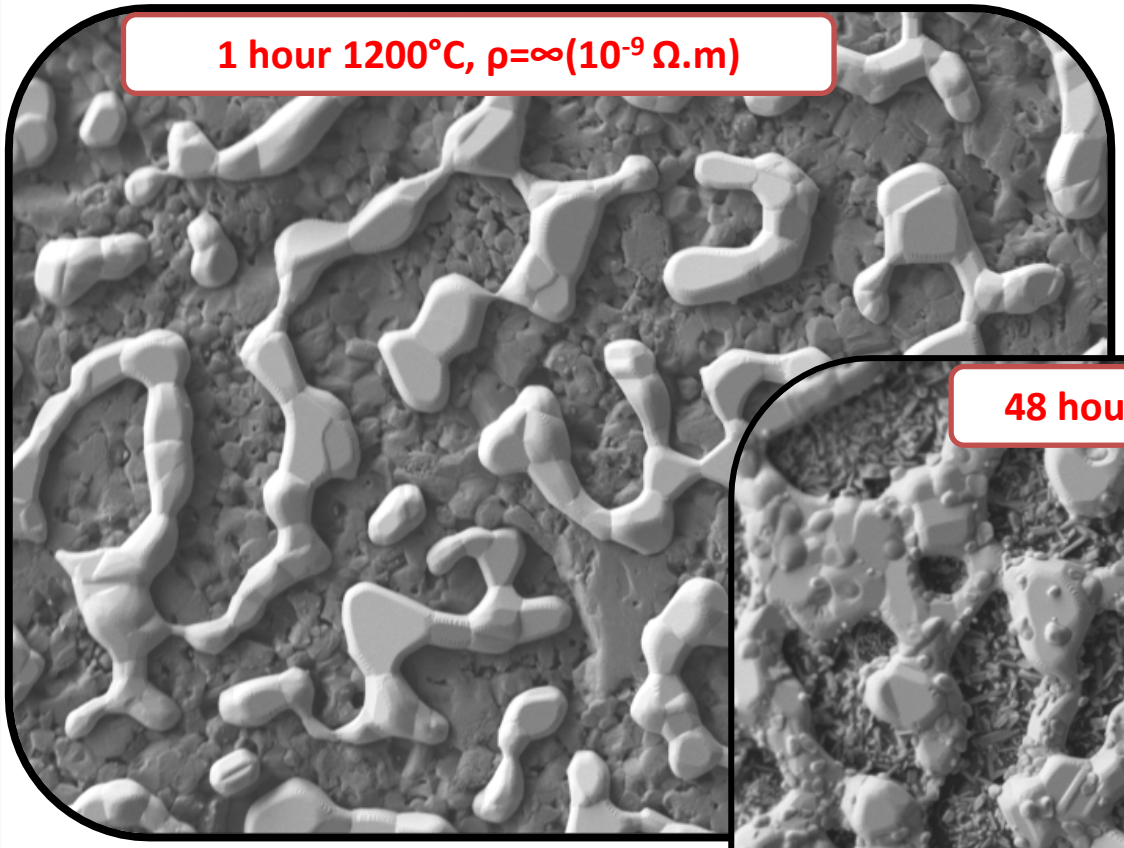

Pure Pt

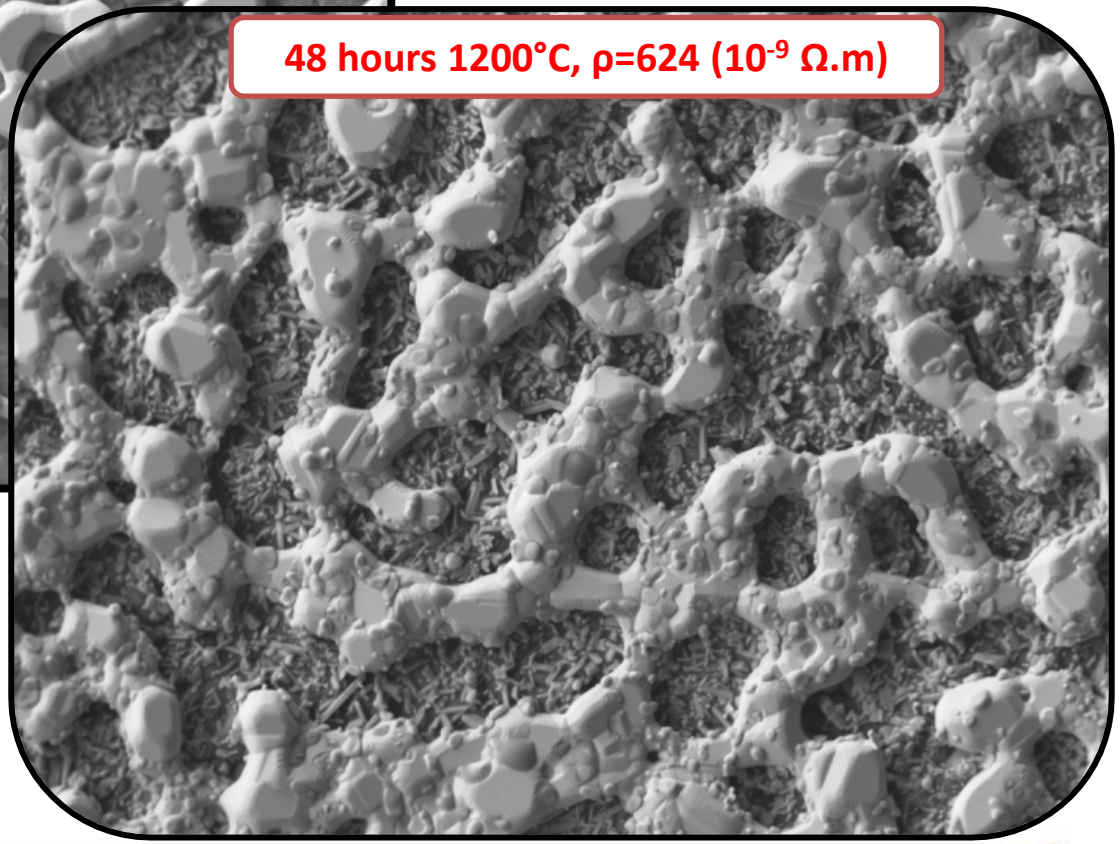

Hf+L-Zr+Pt

Summary: High-Temperature Electrode

Simple Lift-off process for electrode manufacturing.

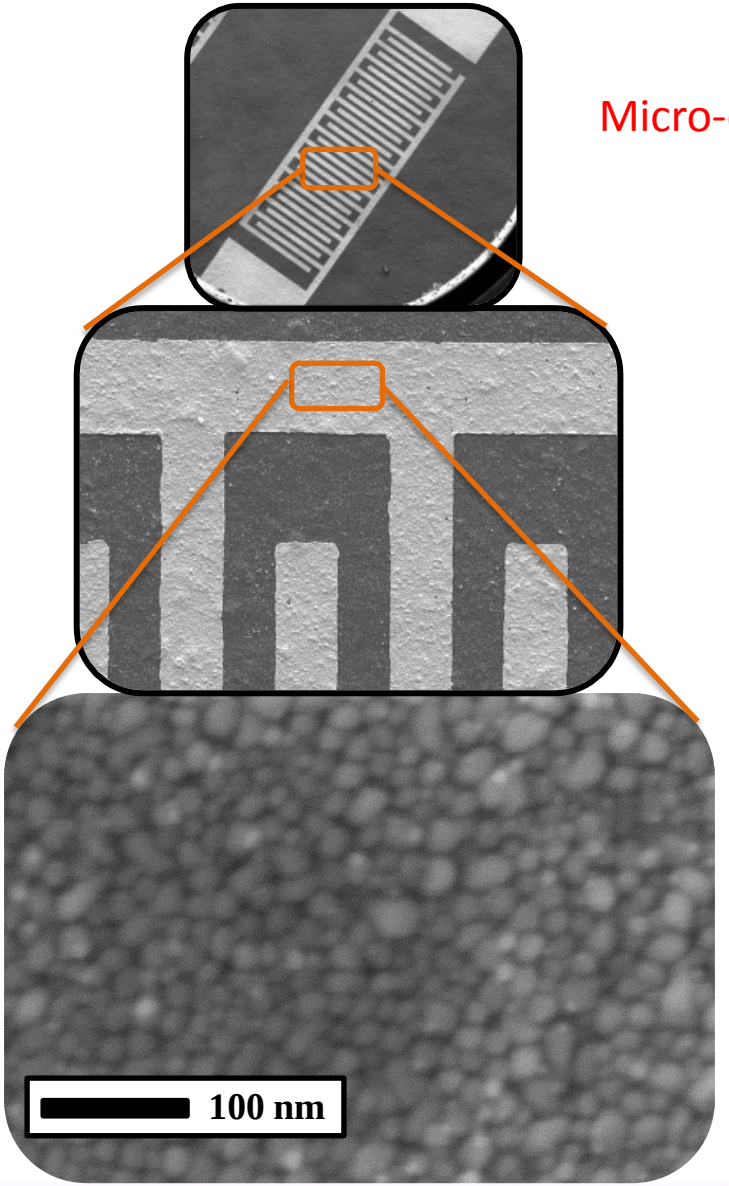

Micro-Sensor Testing

(10%-SnO_2-90%-$Gd_{1.8}Y_{0.1}Zr_2O_7$)

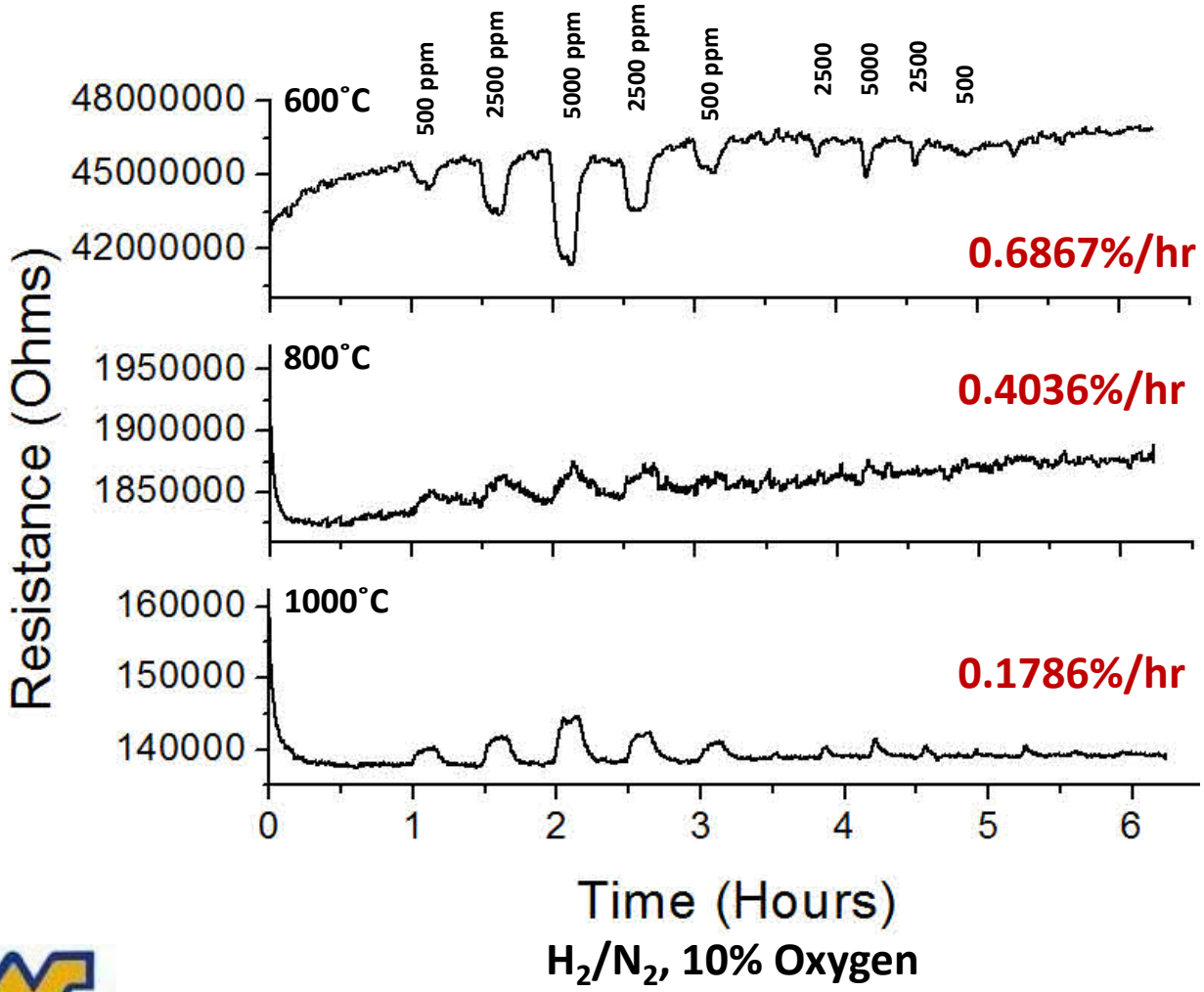

H_2/N_2, 10% Oxygen

- Micro-sensor shows higher sensitivity to H_2 and more stability than macro-sensor.
- Response time also decreases at higher temperature

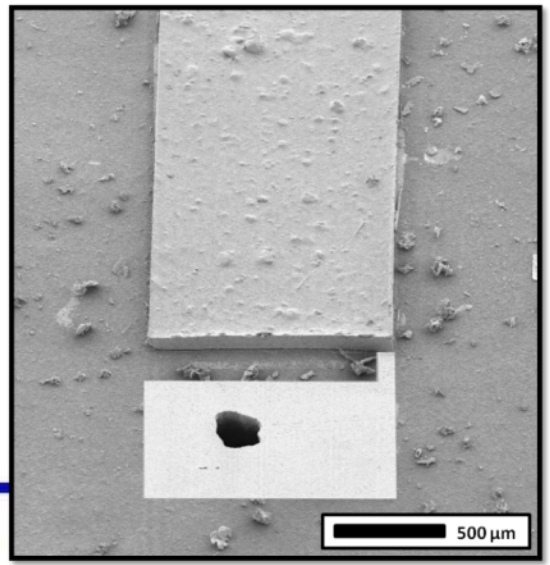

Micro Casting of SnO_2

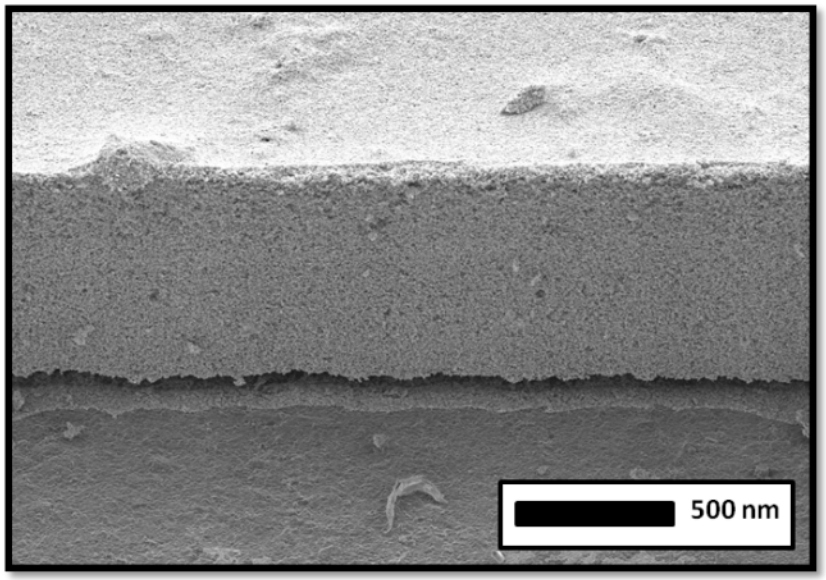

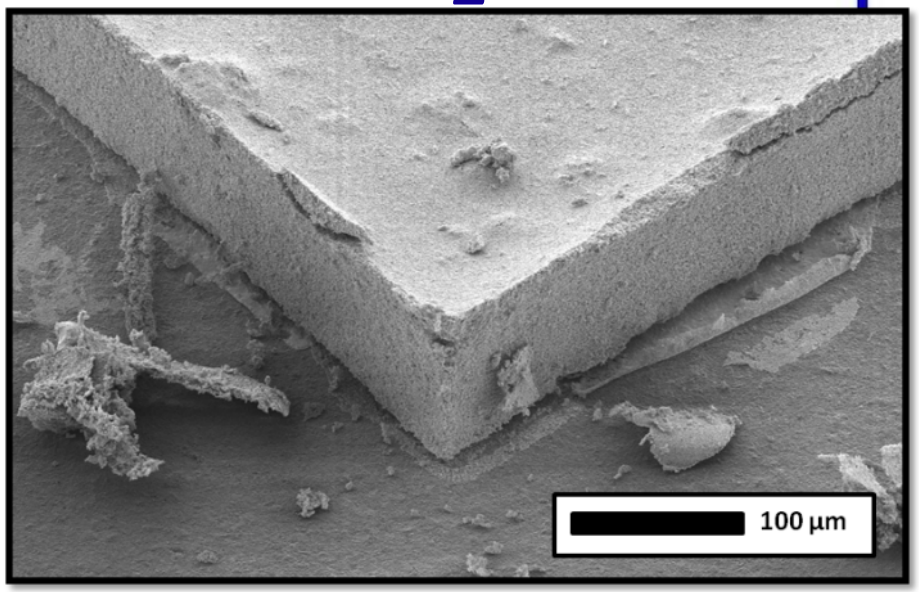

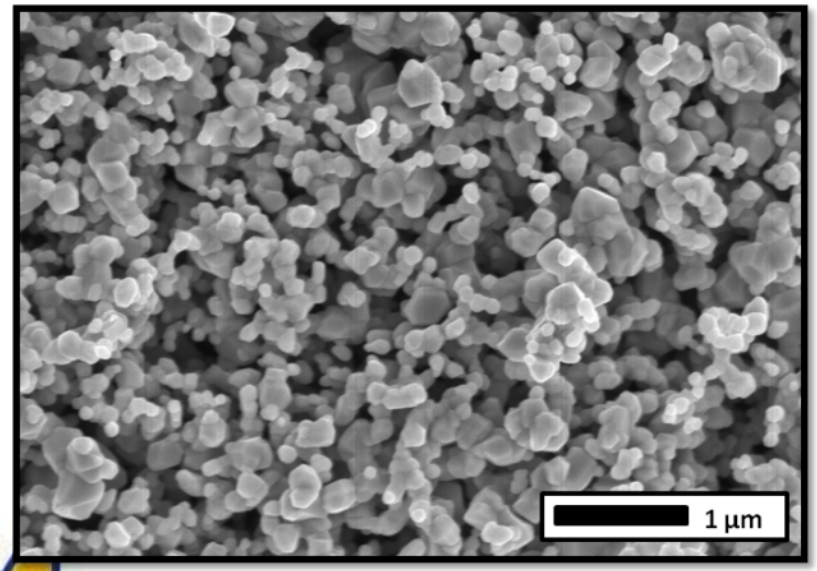

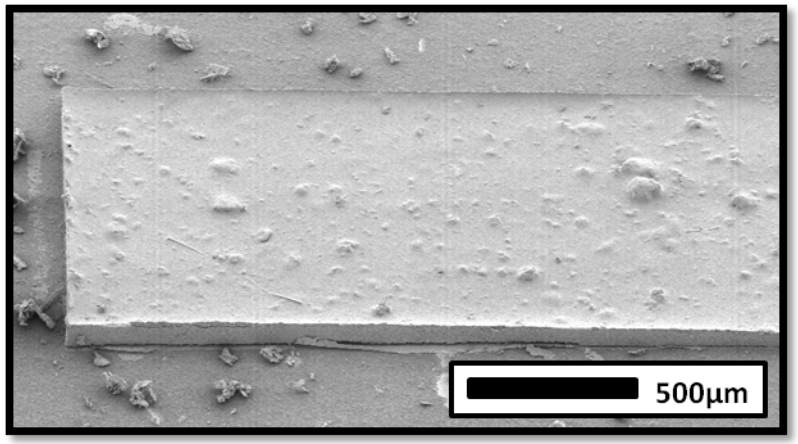

Summary

- Hydrothermal processes for synthesis of ionic and mixed-conducting zirconate, stannate, and titanate pyrochlores (3-10 nm).
- Screenprinted macro-sensors of composite nanomaterials sense 500-4000 ppm H_2 (in air) at 600-1000°C.
- Zirconate and MOS/zirconate composites displayed enhanced stability
  - From 0.792%/hr to 0.016%/hr
- Developed Pt-based micro-IDEs that are stable to 1200°C.
- Initiated development of micro-casting, templated hydrothermal, and DPN processes for fabricating micro-sensor arrays.

Future Work

- Impedance testing to further understand conduction mechanisms of sensing materials
- CO cross-sensitivity testing
- Synthesis and test materials for NO_x sensing
- Co-Sputter deposition of adhesion material with platinum in order to obtain infinite layer structure and characterization
- AEM and TEM characterization for further information about Hf+L-Zr+Pt.

Acknowledgments

- Funding by US Department of Energy, University Coal Research (UCR) program under contract DE-FE0003872.
- Adrienne McGraw, Zachary Santer
- Oak Ridge Institution for Science and Education (ORISE)
- ORAU (Oak Ridge Associated Universities)
- WVU Shared Research Facilities.
- The authors also would like the acknowledge Dr. Kolin Brown, Dr. Wei Ding. Mr. Harley Hart for their assistance.

Additional Information

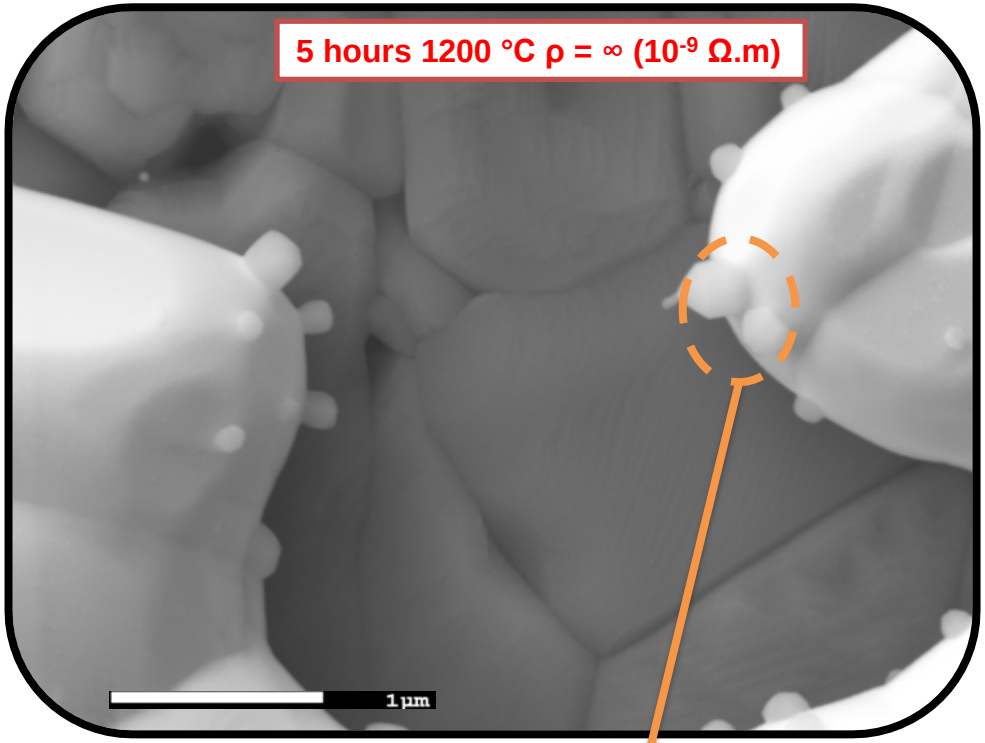
5 hours 1200 °C ρ = ∞ (10-9 Ω.m)
1 µm

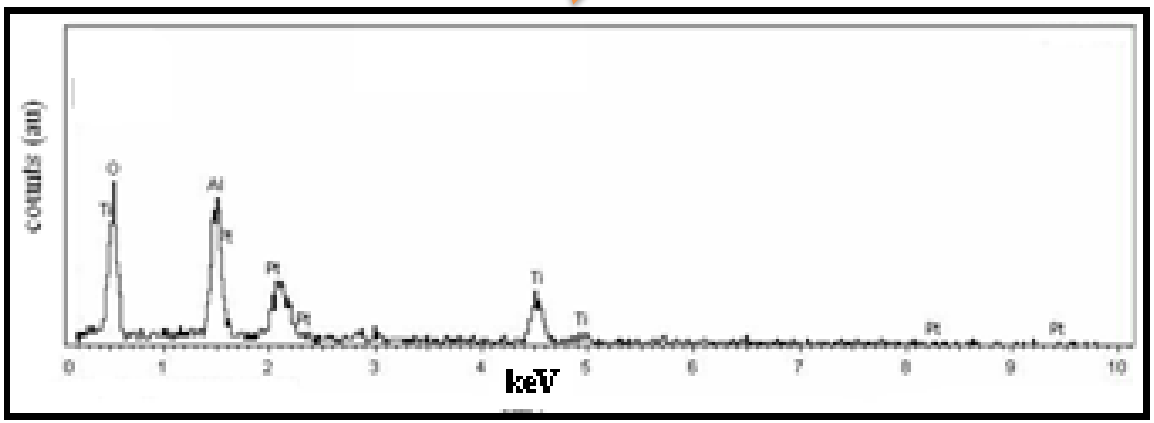
counts (au)
keV
0
1
2
3
4
5
6
7
8
9
10

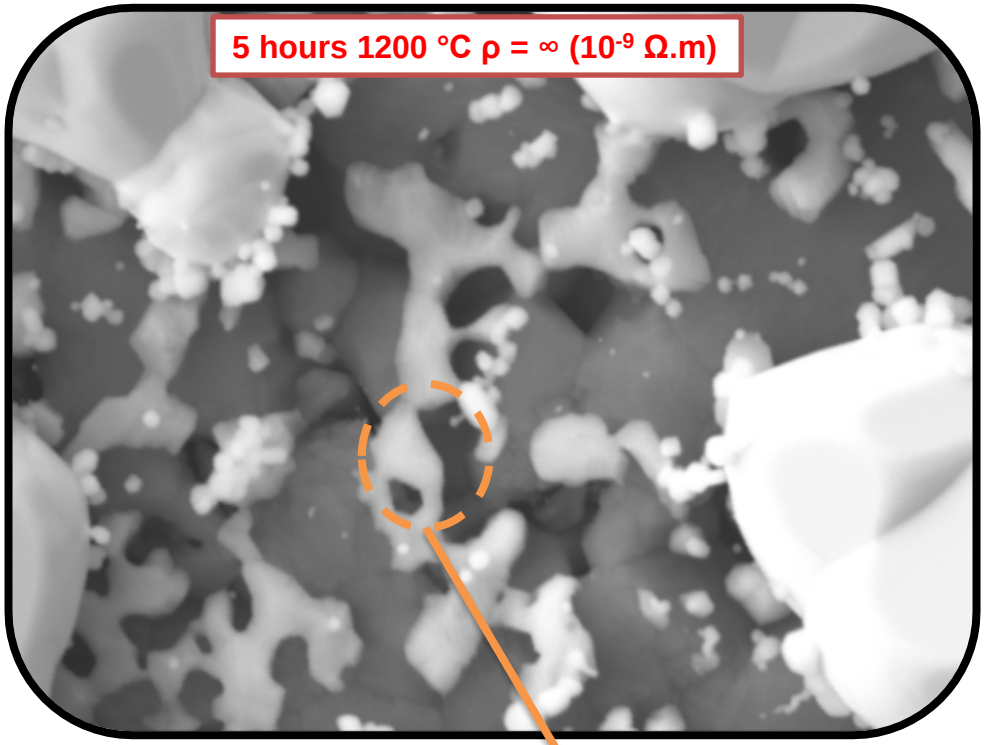
5 hours 1200 °C ρ = ∞ (10-9 Ω.m)

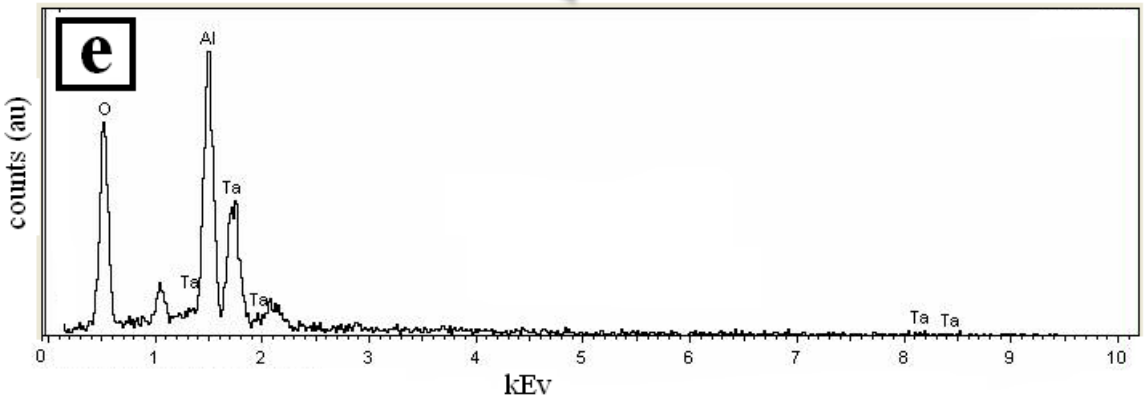
e
Al
O
Ta
Ta
Ta
Ta
Ta
counts (au)
0
1
2
3
4
5
6
7
8
9
10
kEv

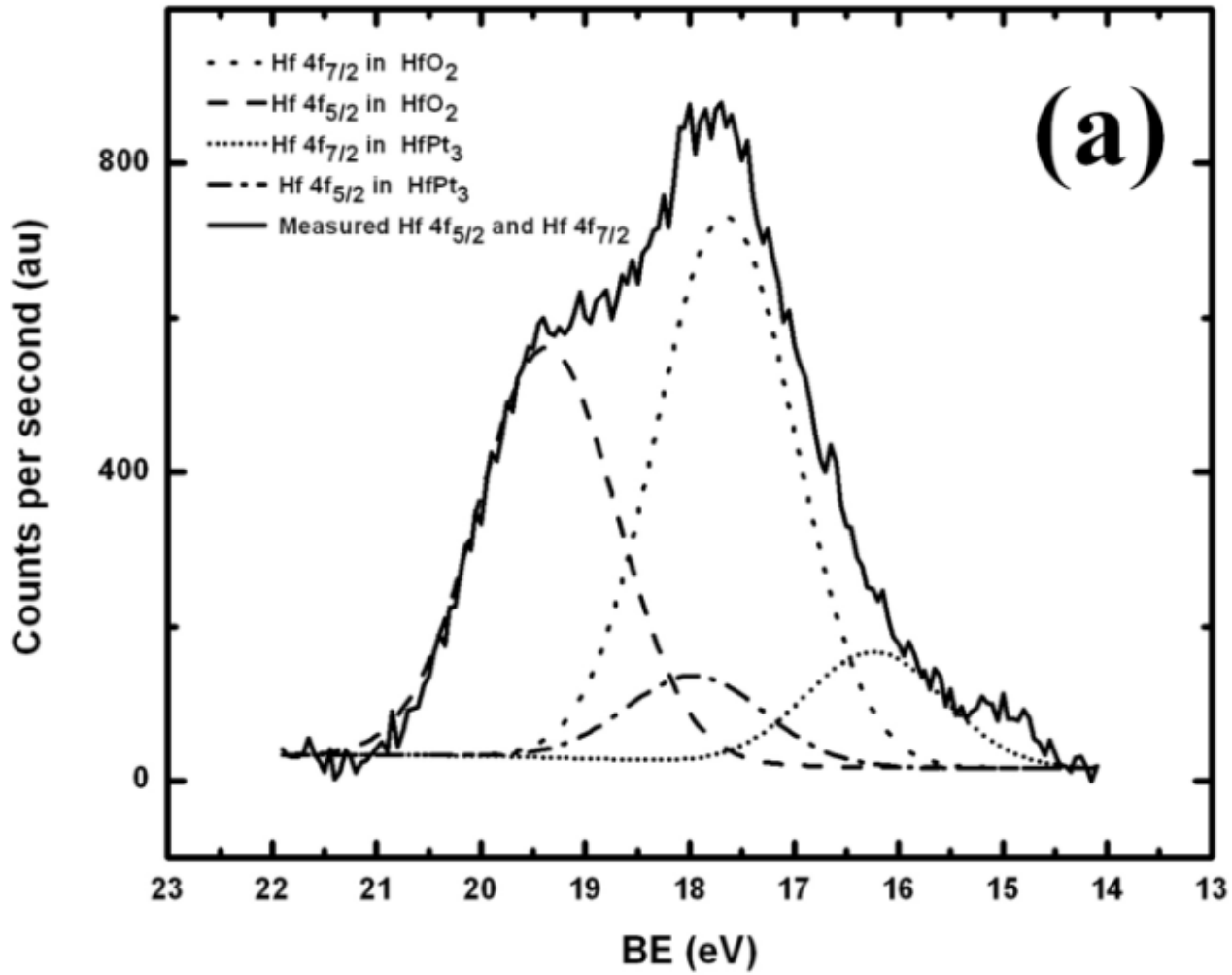

Detailed XPS scan for the **(a) Hf 4f peak positions in the Hf/L-Zr+Pt sample (b) Zr 3d peak positions in the L-Zr+Pt sample, both annealed at 1200°C for 48 h.**

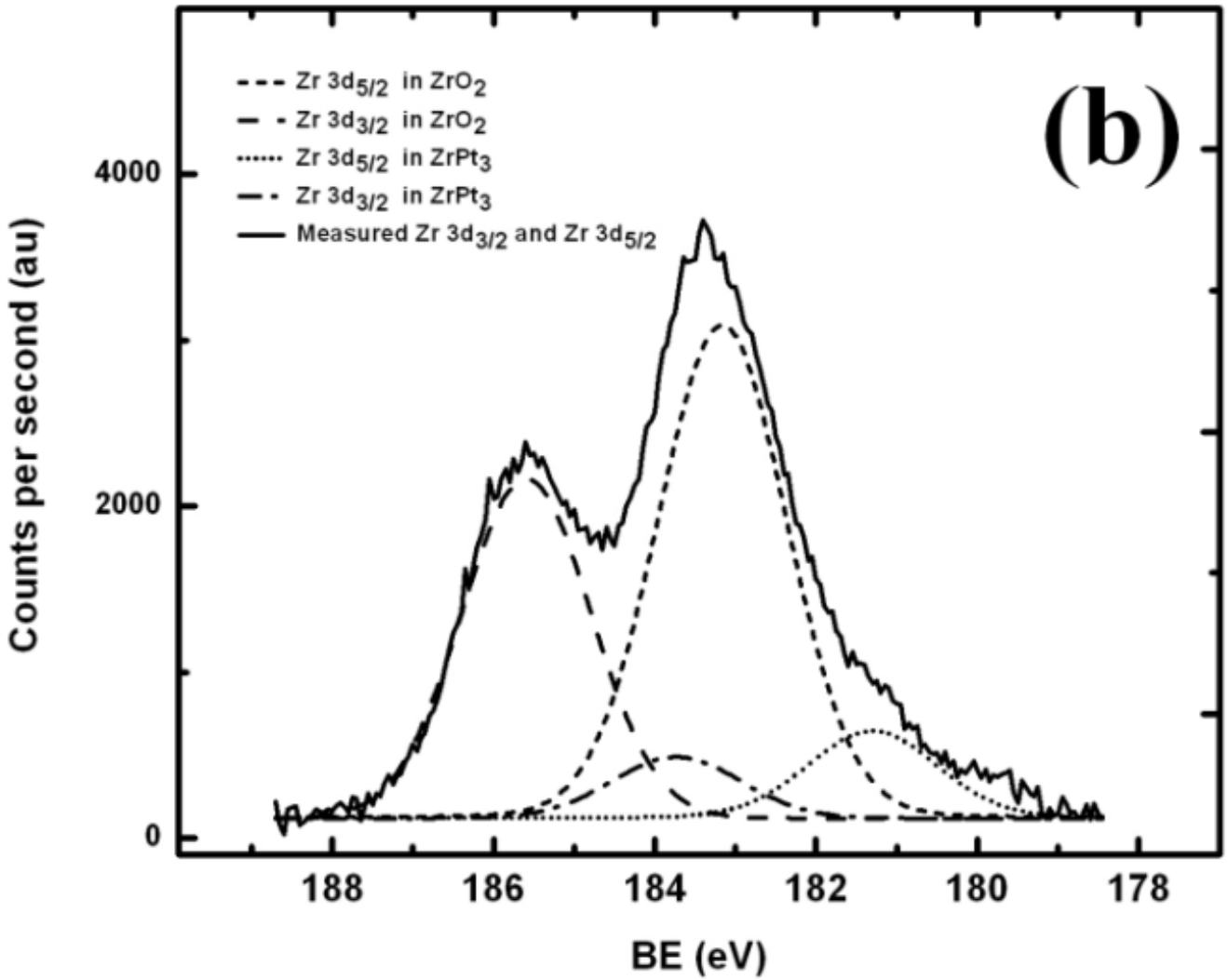

Detailed XPS scan for the **(a) Hf 4f peak positions in the Hf/L-Zr+Pt sample (b) Zr 3d peak positions in the L-Zr+Pt sample, both annealed at 1200°C for 48 h.**

Room temp. sputtering with possible lowest power and highest possible pressure to maximize the mean freem path

Transition Region

Highest possible sputtering temperature, lowest possible sputtering pressure

Compositional Testing ($Gd_{2-x}A_xZr_2O_7$)

$Gd_{1.8}Y_{0.1}Zr_2O_7$

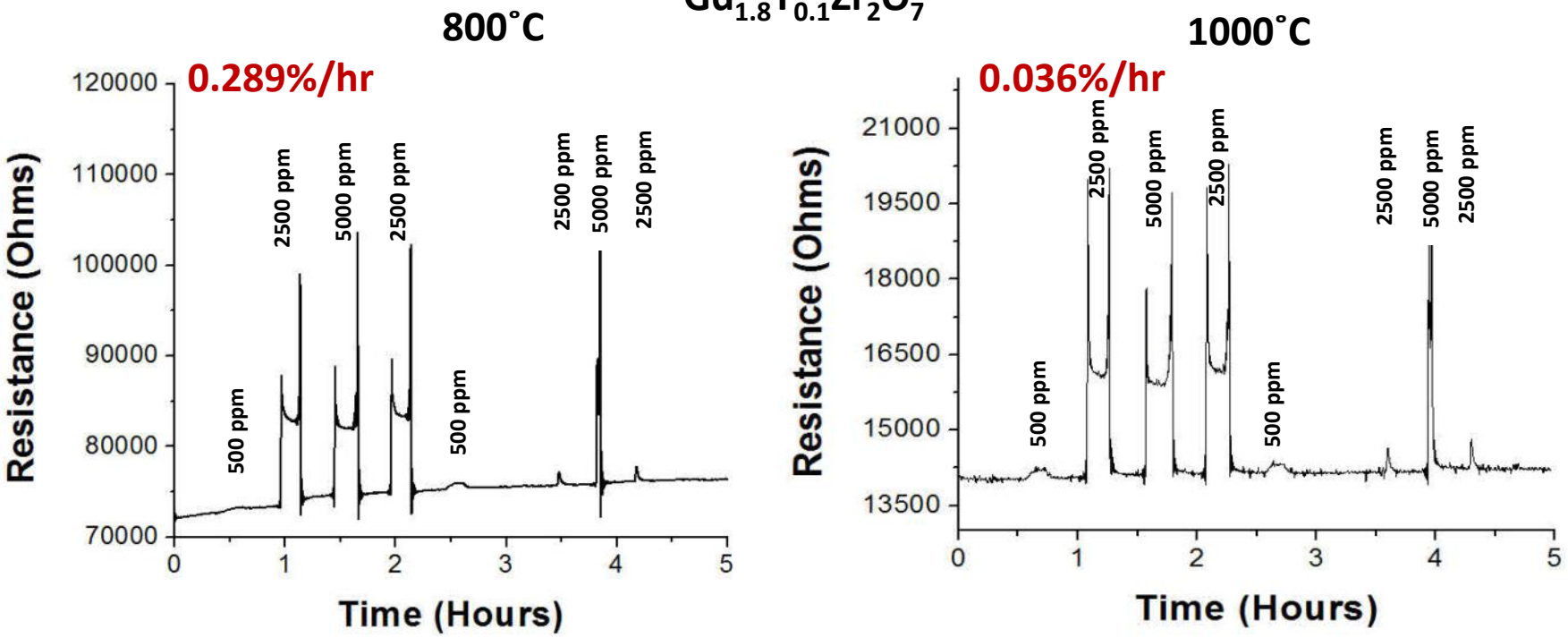

H_2/N_2, *0% Oxygen, 0% Humidity*

- Sensitive to H_2 down to 500 ppm level with less than 1 min response time.
- Surface defect state altered in reducing atmosphere (response independent of H_2 concentration).
- Spike in resistance due surface reduction and stabilization due to bulk oxygen movement and reordering at surface/junction?